INSTITUTE OF
PAPER CHEMISTRY
Appleton·Wisconsin

A STUDY OF DYNAMIC COMPRESSION

Project 3258

Report Two
A Progress Report
to
MEMBERS OF THE INSTITUTE OF PAPER CHEMISTRY

July 1, 1976

THE INSTITUTE OF PAPER CHEMISTRY

Appleton, Wisconsin

A STUDY OF DYNAMIC COMPRESSION

Project 3258

Report Two

A Progress Report

to

MEMBERS OF THE INSTITUTE OF PAPER CHEMISTRY

July 1, 1976

TABLE OF CONTENTS

INTRODUCTION

The two specific objectives of this project on wet pressing are (1) to establish the dryness of wet paper under rapid compression, and (2) to assess the extent of rewetting in subsequent expansion. In the ad hoc meeting held in March, 1975, and in Report One issued by the following June, a review of the dynamics of wet pressing was undertaken, in which we summarized the complexity of this apparently simple operation.

In the course of the review, we suspected that a large part of the conflicting evidence and its diverse interpretations in the literature on pressing could arise from uncontrolled tests. In this project, therefore, we proposed to begin with a definitive study of dynamic compression, experimentally by use of a simplified system and analytically with the aid of a mathematical model. This report deals with the initial results of the compression study.

Based on our previous experience with the static compression of fiber mats, we deemed it necessary to choose a well-defined system for initial dynamic experiments. Our work has been so far restricted to filtration-formed and mechanically conditioned thick mats of dacron fibers confined in a cylinder between a stationary plate and a pneumatically driven permeable piston. During the compression the force on the piston, the fluid pressure at the mat-plate interface, and the mat thickness can be continuously monitored.

The experimental system possesses the following simplifications for the purpose of this study:

1. The dacron fibers have nearly uniform properties. In addition, they are practically nonswelling.

THE INSTITUTE OF PAPER CHEMISTRY

Appleton, Wisconsin

A STUDY OF DYNAMIC COMPRESSION

SUMMARY

A filtration-formed, mechanically conditioned, and water-saturated thick mat of dacron fibers was compressed in a piston press under a schedule of rapid pressure rise.. During the compression the applied pressure, the mat thickness, and the hydraulic pressure were continuously recorded on a light-sensitive chart. The three traces were read into digital data. The data of mat thickness were used to correct the applied pressure for piston inertia. The corrected applied pressure schedule, together with the static compressibility and the Darcy permeability of the mat, was fed into a mathematical model for wet pressing to predict mat thickness and hydraulic pressure.

The predicted thickness was 2-13% lower than the data in the first 40 milliseconds (ms) of compression. A comparison of the predicted and measured hydraulic pressure showed very similar patterns of rise and fall. The data, however, lagged behind the predictions by approximately 5 ms. The first peak of the predicted curve was about 30% lower than the measured value. These discrepancies were attributed to the use of static compressibility in the model.

This study has firmly established the validity of the compression-flow interaction concept. Our mathematical model is capable of accounting for the effect of flow resistance on water removal provided the dynamics of mechanical compression itself can be adequately described. The load-deformation-time behavior of wet paper holds the key to the ultimate effectiveness of pressing, whatever the type of press or felt may be used.

2. The filtration-formed and mechanically conditioned mats have fairly stable and reproducible structures with respect to their compressibility and permeability.

3. The flow of water out of these mats is unidirectional.

The instrumentation for measuring and recording the data meets the following requirements: (1) fast responses, (2) sufficient precision, and (3) little drifting. The measurement of fluid pressure without the interference of fibers has been successfully developed in this project.

Mathematical modeling for a complex process is at best a simulation of reality. Its main uses are (1) to serve as guidance in analyzing experimental data, and (2) to aid a parametric investigation of a practical system when only limited information is available. The present model for wet pressing is based on the concept of dewatering a compressible fiber mat, developed at the Institute more than a decade ago. It is a macroscopic description of the interaction of compression and flow in successive equilibrium states, and has the inherent power of prediction if (1) the information of compressibility and permeability is available, and (2) the initial and boundary conditions are presecribed.

EXPERIMENTAL

COMPRESSION APPARATUS AND INSTRUMENTATION

The compression apparatus (Fig. 1) consisted of a 3.00-inch (I.D.) cylindrical cup mounted on a flat plate, into which was inserted a permeable piston. The component parts were made of brass, and all contact surfaces were machined. The top of the piston was connected with a driving member by a ball-adapter joint to facilitate self-alignment. The driving member was a rod attached to a flexible diaphragm sealed in an air chamber which was connected with a compressed air source and the atmosphere through two quick-opening valves. The piston proper contained a number of evenly distributed fluid channels with a fluid reservoir in its midsection. The lower face of the piston was covered with a 35-mesh backing screen and a 100-mesh facing screen. The complete apparatus was mounted in a heavy frame on a rigid base.

The force acting on the piston by compressed air was measured by a strain-gage load cell mounted between the adapter and rod. The hydraulic pressure was monitored with a miniature pressure transducer imbedded in the plate about 1/4-inch deep and facing upward. Four small pressure taps drilled through the face of the plate were connected by a horizontal passage to the transducer to prevent the sensing element from direct contact with fibers. The piston displacement or mat thickness was measured with a linear motion potentiometer. This thickness gage mounted vertically on the base was attachable to the piston with a swing arm. The three signals were transmitted to a Honeywell Accudata Multichannel DC amplifier and traced optically on a Honeywell Viscorder Oscillograph.

The response of the instrumentation from the sensing element to the recorder was limited by the latter which was specified to have a step response

Compressed Air

Quick Opening Valves

Air Chamber

Diaphragm

Driving Rod

Protector

Strain Gage Load Cell

Connecting Arm for
Thickness Gage

Adapter

Ball

Reservoir

Cup

Piston
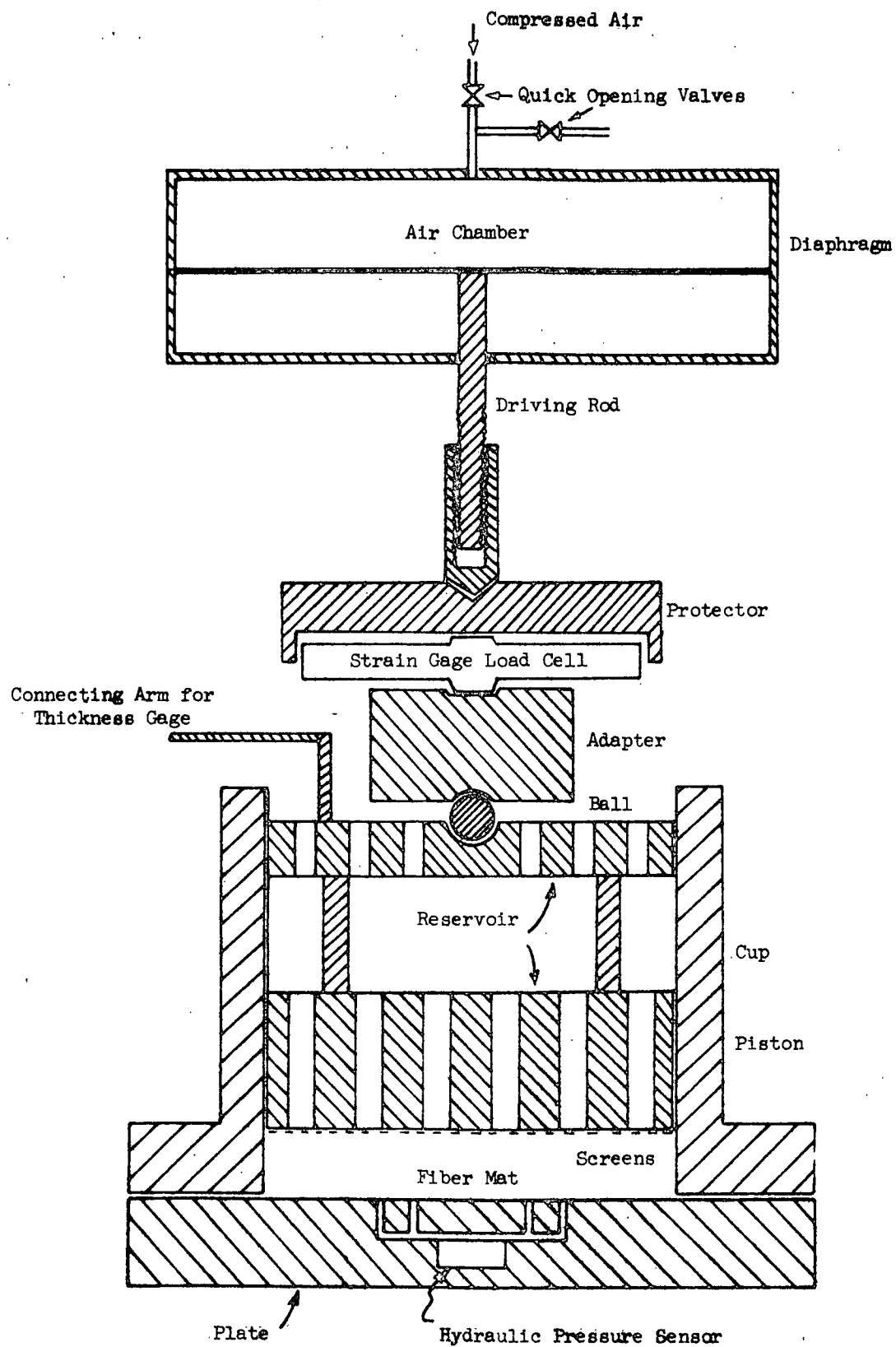
Screens

Fiber Mat

Plate

Hydraulic Pressure Sensor

Figure 1. Sketch of Compression Apparatus

of 0.2 ms. This was verified for each of the three channels by applying an input from a pulse generator and observing the time elapsed for the output. The pulse, a step function, could be generated in a few µs, and the observed time of response agreed with the specified limit.

The galvanometers in the recorder, one for each channel, were checked for linearity by measuring known thicknesses of a set of spacers with the linear motion potentiometer and recording the output on a chart. It was found that all three channels responded linearly.

Finally, the sensing devices were calibrated against a pressure gage, a mercury manometer, and a micrometer. The resulted calibrations were all linear.

PREPARATION OF FIBER MAT

The fibers were prepared from a yarn of dacron monofilaments with a razor-band cutter. The average length was measured to be 3.65 mm and the average diameter 23.1 µm. The dacron fibers have a density 1.38 g/cm^3.

The fiber bundles were readily dispersed in hot distilled water under a vacuum. The dispersed fibers were diluted to 0.1 g/liter with distilled water, and formed by filtration into a mat about 2 cm thick in about 40 min to reach a basis weight about 2000 g/m^2. The water-saturated mat was transferred, with the support of a plastic film, onto the plate of the compression apparatus. After the mat was properly centered, the cup was replaced, and the piston lowered on the mat.

The maximum air pressure desired for dynamic compression was applied to the mat for 2 min. The pressure was then released, and the mat allowed to expand and remain water-saturated under the weight of the piston (1576 g) for 2 min.

This compression-recovery cycle was repeated 12 times. The mat was thus "mechanically conditioned."

After a dynamic compression test, to be described later, the wet mat was removed and dried overnight in an oven at 105°C. The dry mat was weighed and replaced on the plate for mechanical conditioning again.

STATIC AND DYNAMIC COMPRESSION TESTS

The static test for both wet and dry mats was performed in the compression apparatus. The mat thickness under a constant load for 15 min was measured in the pressure range of the dynamic test.

In a dynamic test, a mat was compressed in a time of the order of 10^2 ms to a maximum pressure of about 5×10^7 dyne/cm^2 (700 psi). With the manual manipulation of the air valves, the rate of pressure change could not be precisely controlled. During the run, the applied load, the hydraulic pressure, and the mat thickness were traced as functions of time on a linear chart.

After the mat was removed, the zero readings for applied force and hydraulic pressure were recorded on the same chart. The piston was then lowered to contact the plate, and the zero reading for thickness was also noted.

Next, a load, usually 100 psi, was applied to the stationary piston, and calibrated against a pressure gage. Following this step, the piston was lifted to a certain position from the plate, and the clearance was calibrated against a micrometer. Finally, the space between the piston and the plate was confined by a special rig and completely filled with water. A small pressure was applied to the piston and calibrated against a mercury manometer. All of these calibrations were noted on the same chart.

The light-sensitive chart was photographed without appreciable distortion to yield a negative film. By the use of a microcomparator, the traces in the film were read into digital data at chosen time intervals.

PERMEATION APPARATUS AND TEST

A sketch of the permeability apparatus is shown in Fig. 2. A mechanically conditioned and water-saturated mat was clamped and sealed between two permeable septa at a prefixed clearance. Distilled water, deaerated and filtered, was forced through the compressed mat at a slow rate under a pressure drop amounting to only a small fraction of the compressive stresses sustained by the mat. The flow rate, pressure drop, and water temperature were measured.
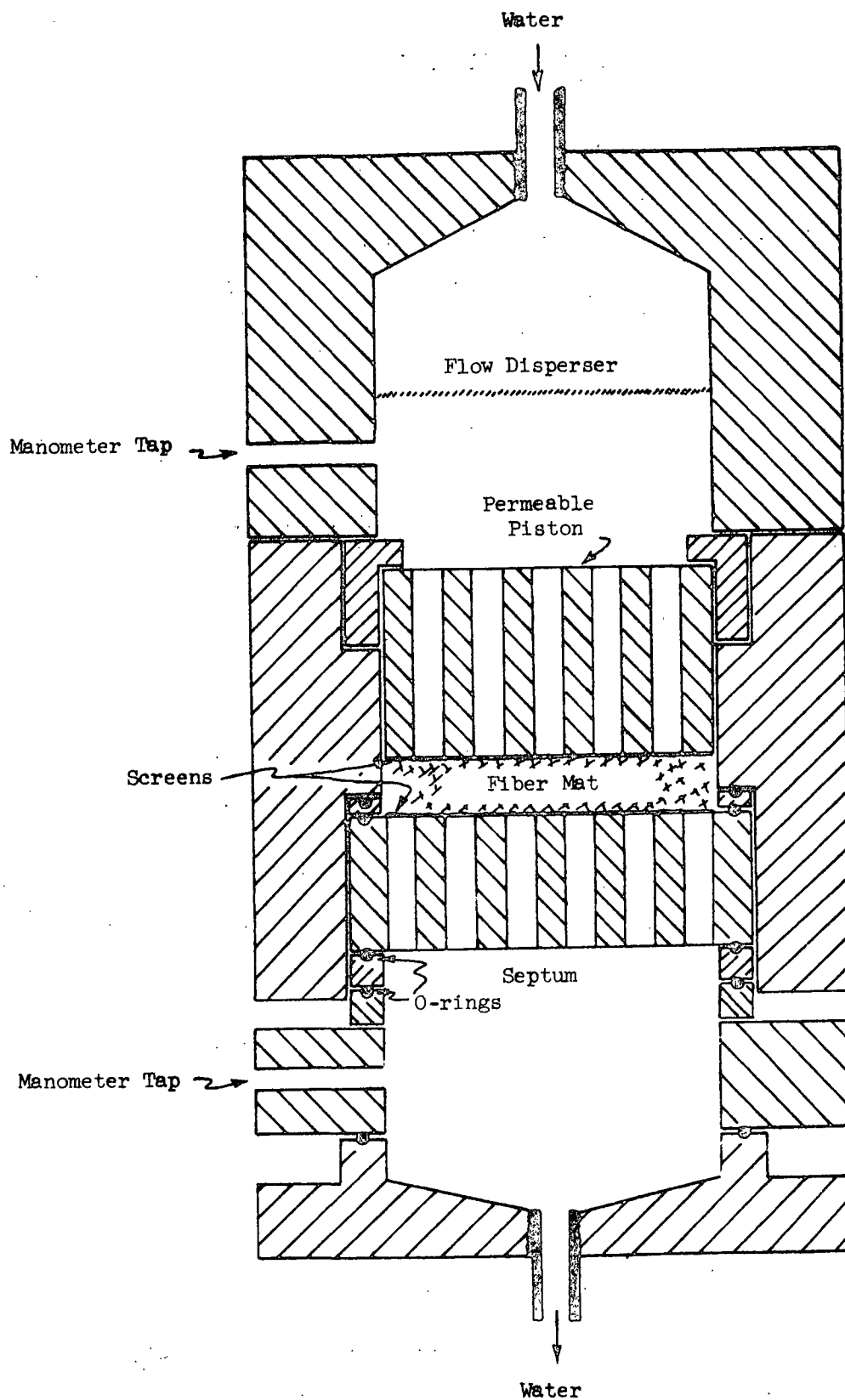
Water

Flow Disperser

Manometer Tap

Permeable
Piston

Screens

Fiber Mat

Septum

O-rings

Manometer Tap

Water

Figure 2.   Sketch of Permeation Apparatus

CORRELATION OF DATA

COMPRESSIBILITY

Ingmanson's work ($\underline{1}$) on the compressibility of filtration-formed mats of synthetic and cellulosic fibers at low pressures (10^3-10^5 dyne/cm^2) for relatively long times (10^3 sec) supported the use of the power law:

$$c - c_o = Mp^N \qquad (1)$$

where $\underline{c}_o$ is hypothesized as the mat density at zero stress. For the first compression, $\underline{c}_o$ is 0.02-0.04 g/cm^3, about the sedimentation concentration of a fiber network, $\underline{N}$ in the range of 0.22-0.45, and $\underline{M}$ roughly proportional to $\exp(-\underline{N})$.

Kurath's study ($\underline{2}$) of dry and wet nylon fiber mats under the first compression in the pressure range 10^4-10^9 confirmed the applicability of the power law until a maximum pressure was reached, beyond which the mat density remained constant. The transition from variable to constant density was not exactly sharp. The wet mat attained a maximum density of 1.0 at a pressure of 3.8×10^8, as compared with the nylon density of 1.106. Above a pressure of 10^7, fiber damage (permanent set) in contact areas was readily visible under a microscope.

Kurath also found that the dry mat at high pressures showed the same value of $\underline{N}$ as the wet mat, but a lower value of $\underline{M}$. This reduction of compressibility from the wet to dry state may be attributed to a decrease of fiber conformability (flexibility and plasticity) as a result of deswelling ($\underline{3}$).

Wilder ([4]) investigated the creep of wet wood fiber mats at low pressures. He correlated his data for both freshly formed and mechanically conditioned mats by

$$c - c_o = (M_1 + M_2 \log t)p^N, \qquad (2)$$

where M_1 and M_2 are both positive for compression. N was found to be independent of time, and M independent of pressure.

Wilder's analysis of his short-time (<0.1 sec) compression data demonstrated that the rate of mat deformation was controlled by the resistance of the mat structure to the flow of water, and dependent little on creep. The current understanding of wet compression in a transversal-flow press ([5]) is in general agreement with this finding.

The static compressibility data for the wet and dry mats of dacron fibers in this study were correlated by the power law. The smooth curves in Fig. 3 represent the computed correlations with the values of the parameters listed in Table I.

TABLE I

STATIC COMPRESSIBILITY FUNCTIONS

Mat	c_o	N, cgs units	M	Max. Deviation, ±, %
Wet	0.2231	0.2360	0.007291	3.8
Dry	0.1544	0.1701	0.02171	2.5

It is noted that for these mechanically conditioned mats, c_o is considerably larger and N appreciably smaller than those for the first compression ($c_o \approx 0.03$, $N \approx 0.25$). The hypothetical zero-stress mat density is expected to increase with increasing mechanical work, and a denser initial structure to respond less sensitively to pressure ([3]).
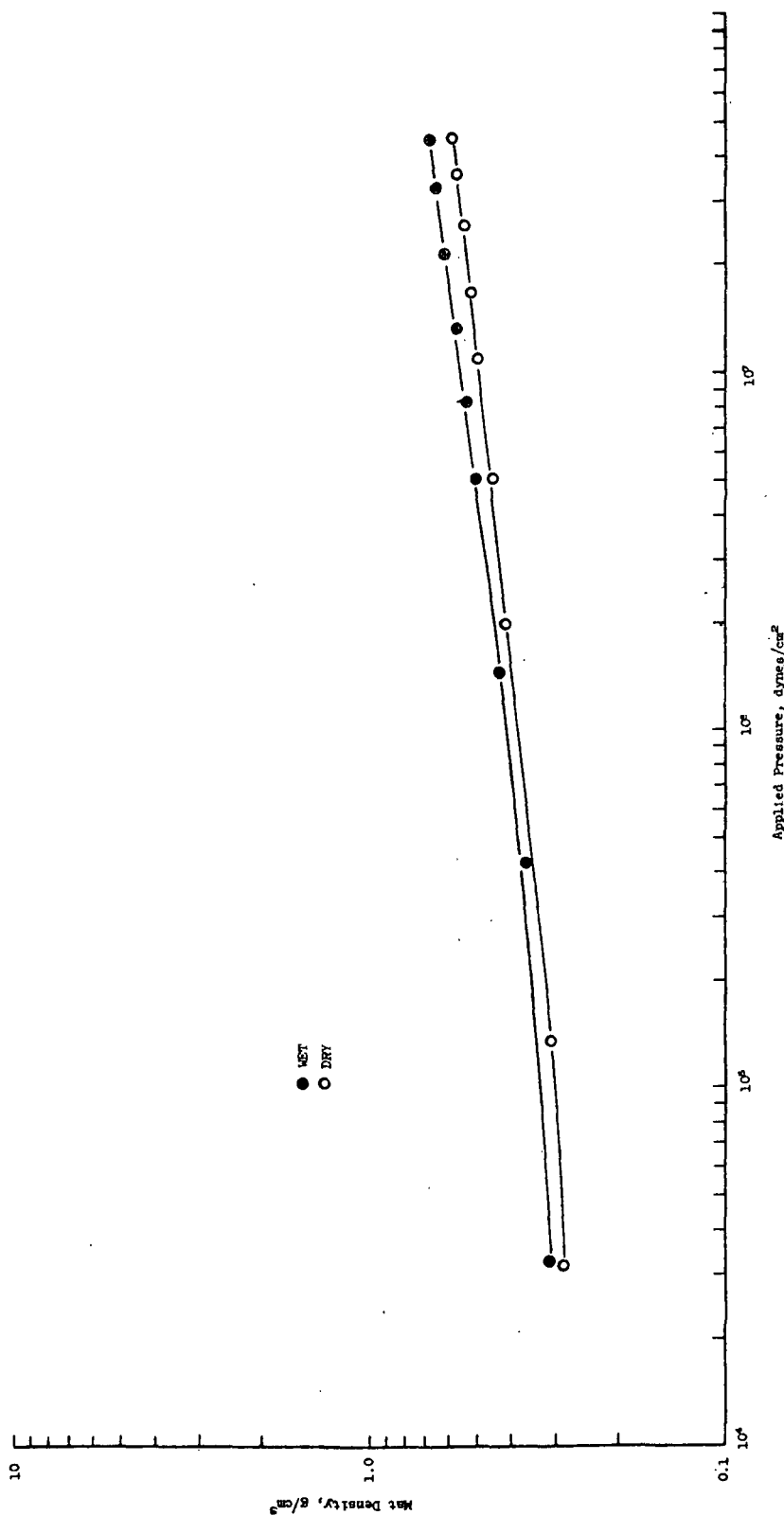
Figure 3.   Compressibility of Dry and Wet Mats

If the maximum mat density is assumed to be approximately 90% of the dacron density, the limiting pressure may be estimated from the compressibility function. The order-of-magnitude of p_{max} is compared with Kurath's nylon data in Table II. It is seen that the higher p_{max} for dacron may be a reflection of its lower fiber conformability involving both elasticity and plasticity.

TABLE II

COMPARISON OF LIMITING PRESSURE

	Dacron	Nylon
p_{max}	10^9	10^8
E	10^{11}	10^{10}

PERMEABILITY

Slow flow through a porous medium follows the Darcy law:

$$U' = \frac{K}{\mu} \frac{\Delta p'}{L} \tag{3}$$

The permeability $\underline{K}$ is a dynamic characteristic of the porous structure. According to the Kozeny-Carmen model,

$$K = \frac{\varepsilon^3}{k S_v^2 (1 - \varepsilon)^2} \tag{4}$$

in which $\underline{k}$, the Kozeny factor, is approximately constant for most incompressible porous media composed of solid particles in a dense packing ($\varepsilon < 0.5$). At high porosities, however, $\underline{k}$ is a strong function of ε for a given porous medium.

A fiber mat may have a very high porosity (> 0.95) in an uncompressed state. It approaches zero porosity as the compacting pressure is increased to the limit. Ingmanson and coworkers ($\underline{6}$) measured the permeability of filtration-formed mats of cylindrical fibers in the porosity range of 0.67-0.96, from which the variation of $\underline{k}$ with ε was correlated under the assumption of constant $\underline{S_v}$.

In wet pressing the porosity varies over a wide range. The permeability of a compressed mat with moderate porosities has not been reliably measured on account of experimental difficulties in septum construction, air entrainment, and permeability decay.

The permeation data for dacron mats in Fig. 4 indicate that (1) the flow is in the Darcy range, (2) the septum resistance is negligible, and (3) there is little permeability decay. From the slopes of these lines the permeability is evaluated at the known mat porosity and water viscosity. A direct correlation of $\underline{K}$ with ε is shown in Fig. 5. Within the experimental range the increase of permeability with porosity is monotonic at ever accelerated rates. An empirical expression for the correlation is computed as

$$K = 6.395 \times 10^{-6}\, \varepsilon^{11.3} + 0.573 \times 10^{-6}\, \varepsilon^{2.34} \qquad (5)$$

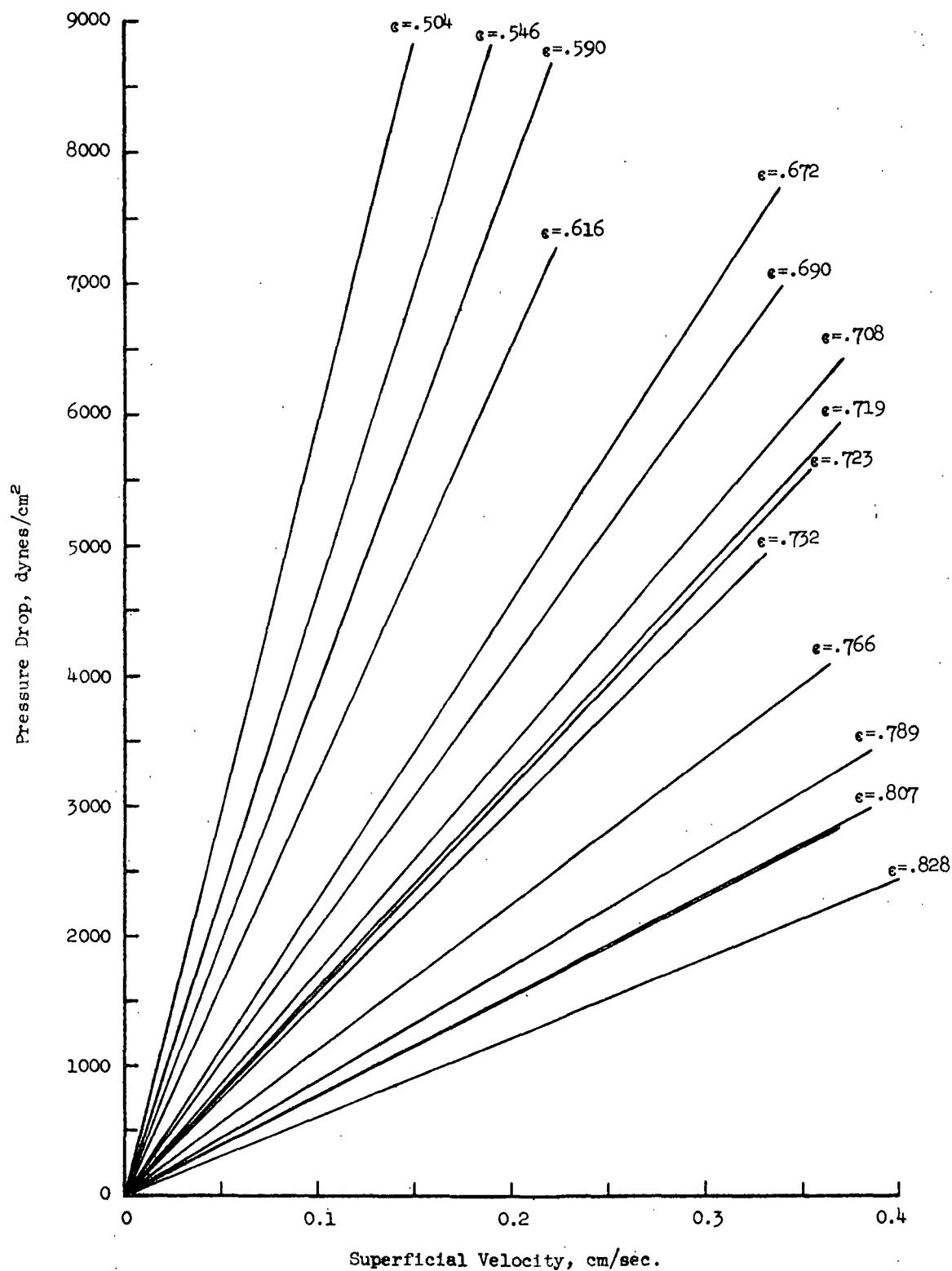where $\underline{K}$ is in cm^2.
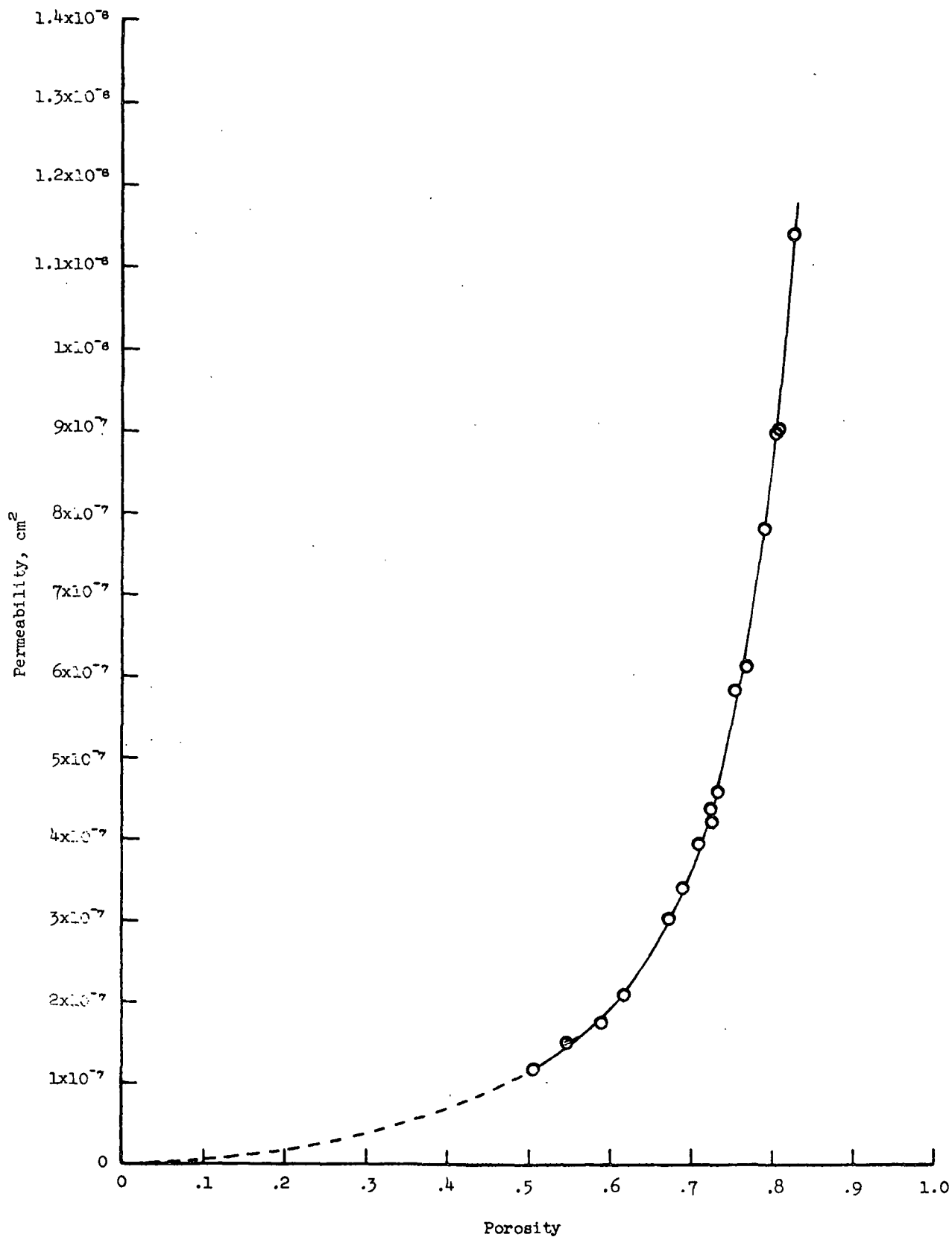
Figure 4.   Permeation Data

Figure 5. Permeability Correlation

DISCUSSION OF RESULTS

COMPRESSION OF DRY MAT

Figure 6 shows the recorded chart for the compression of a mechanically conditioned dry dacron fiber mat. It is apparent at once that the fluid pressure remains unchanged throughout the test. The rise of applied pressure is continuous, but not smooth in the initial period, as a consequence of the manual operation of the air valves.

At this point, the relation of piston motion to compacting pressure should be discussed. If the thickness reduction is nonlinear, the piston cannot be in a uniform motion. When the piston is accelerating, the pressure acting on the mat is less than the measured value. Conversely, the mat experiences a force larger than the apparent load during piston deceleration. This pressure correction may be achieved by a graphical evaluation of the derivatives of the thickness data.

The process of correction is summarized in Table III. The first derivative representing the piston velocity is evaluated from a plot of thickness vs. time (Fig. 7). It is seen that the piston accelerates to a maximum velocity at 14 ms, then decelerates to a minimum velocity at 20 msec, and from there accelerates again. The second derivative multiplied by the mass per unit area of the piston is the amount of pressure correction. The correction at early times is considerable; it becomes insignificant when the point of the minimum velocity is well over. Both the measured and corrected pressure schedules are shown in Fig. 8. It is seen that the correction makes the pressure wiggling more pronounced than the original.
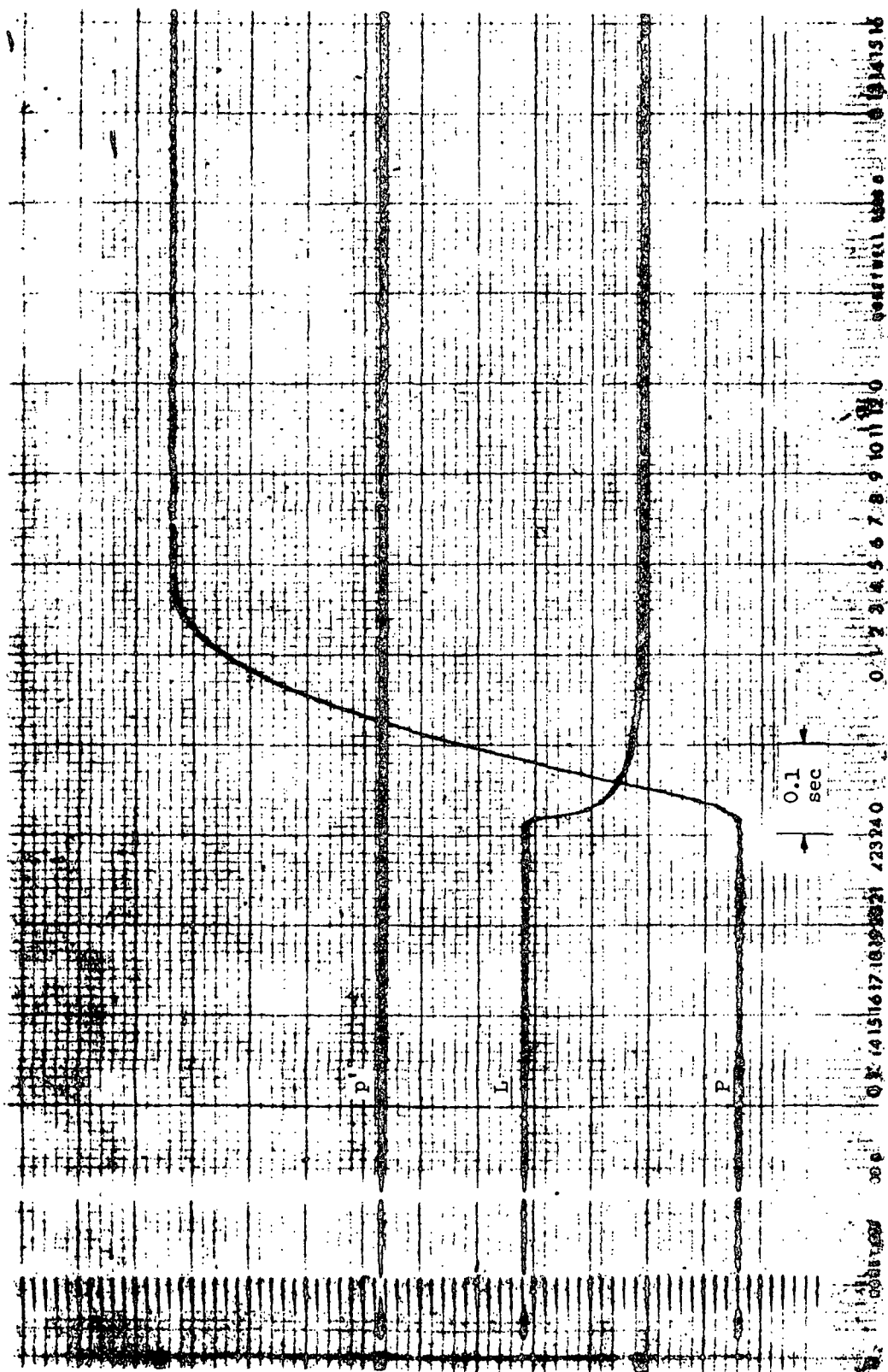
Figure 6. Dry Compression Chart

TABLE III

PRESSURE CORRECTION

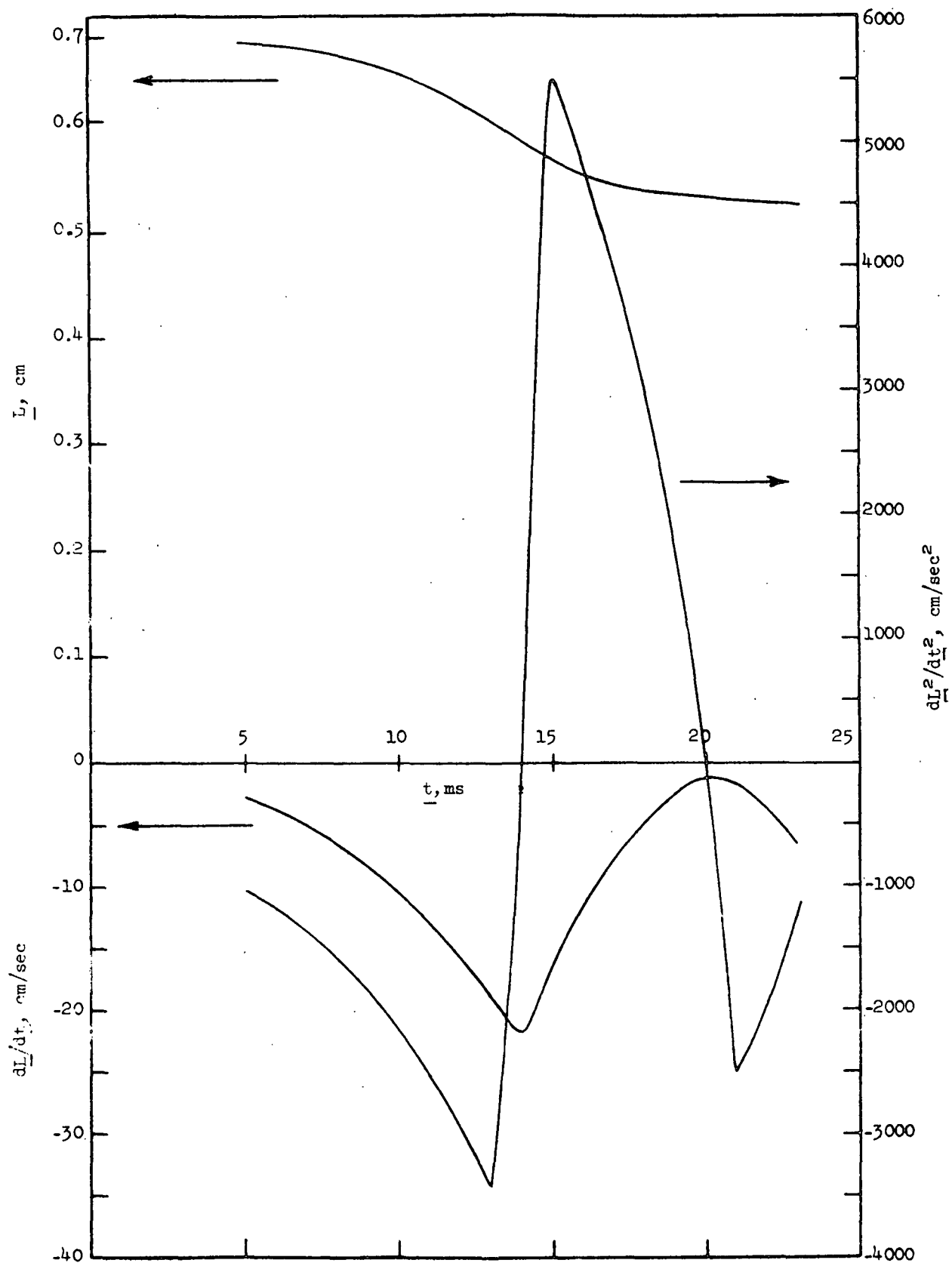| t, sec $\times 10^3$	P, meas. dyne/cm^2 $\times 10^{-6}$	L, meas. cm	$\dfrac{dL}{dt}$, cm/sec	$\dfrac{d^2L}{dt^2}$, cm/sec^2	P, corr. dyne/cm^2 $\times 10^{-6}$	$\dfrac{P, \text{ corr.}}{P, \text{ meas.}}$
0	0.06153	0.6826				
5	0.09968	0.6755	- 2.69	-1010	0.06429	0.645
6	0.1117	0.6735	- 4.04	-1170	0.07133	0.639
7	0.1285	0.6695	- 5.27	-1410	0.08168	0.636
8	0.1535	0.6643	- 6.48	-1640	0.09835	0.640
9	0.2136	0.6558	- 8.25	-1950	0.1461	0.685
10	0.2841	0.6469	-10.67	-2360	0.2056	0.697
11	0.3785	0.6353	-13.12	-2440	0.3046	0.805
12	0.4878	0.6199	-15.48	-2770	0.3919	0.803
13	0.5885	0.6042	-18.40	-3430	0.4728	0.803
14	0.7208	0.5846	-21.84	0	0.7208	1.00
15	0.9048	0.5649	-16.55	+5520	1.096	1.21
16	1.115	0.5532	-11.95	+4430	1.274	1.14
17	1.301	0.5408	- 9.05	+3660	1.436	1.10
18	1.438	0.5356	- 4.74	+2860	1.537	1.07
19	1.512	0.5322	- 2.48	+2410	1.602	1.06
20	1.603	0.5305	-0.743	0	1.603	1.00
21	1.707	0.5282	- 1.42	-2510	1.621	0.882
22	1.839	0.5265	- 4.45	-2000	1.755	0.955
23	2.100	0.5204	- 6.48	-1130	1.991	0.910

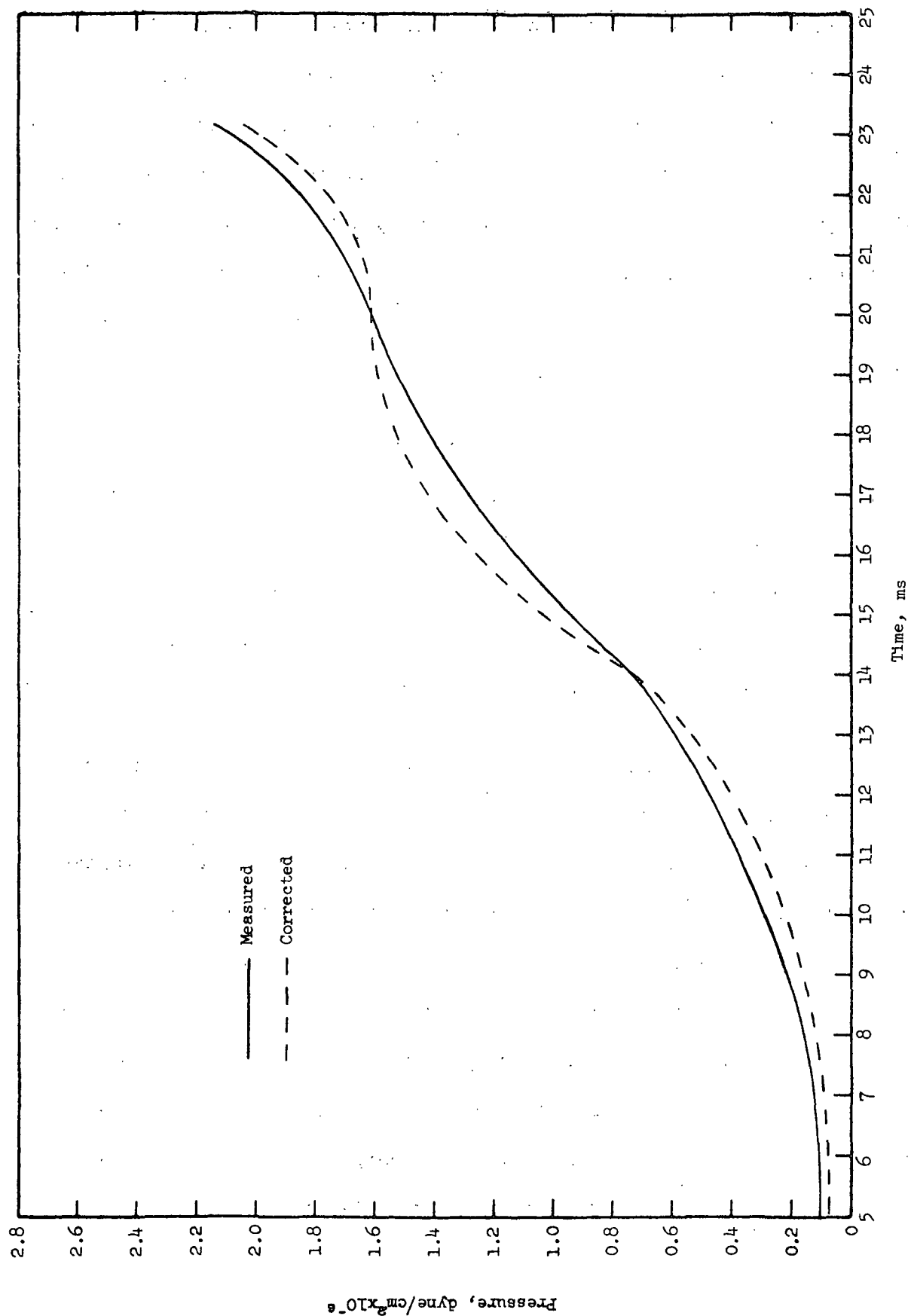Figure 7.   Time Derivatives of Mat Thickness

Figure 8. Pressure Correction for Dry Compression

Without the complication of flow resistance, the compression of the
dry mat is strictly mechanical. The structure of the mat remains uniform
throughout its thickness. The compression test may be considered in two parts:
the dynamic period of rising pressure and the static period of constant pressure.
The second part is usually referred to as a creep test. The creep of a mechan-
ically conditioned dacron mat is very small, as illustrated in Fig. 9. The
increase of mat density amounts to about 0.5% per decade of seconds. Creep,
therefore, will not be further considered.

If it is assumed that the mat were capable of attaining equilibrium
instantaneously, then its thickness would be the same as that calculated from
the static compressibility. In Table IV, the calculated thickness is based on
the corrected pressure. However, because of the low compressibility of the
dacron mat, the uncorrected pressure, if used, will yield only a small difference
in the result of this calculation.

A direct comparison by the ratio of the calculated to the measured
thickness indicates that dynamic compression with a rising pressure is less
effective than static compression at a constant load. The deviation ranges
from 3 to 10% in the first 23 ms. A more meaningful comparison may be made
in terms of mat deformation. The relative deformation, ΔL meas./ΔL calc., is
an indication of how closely the actual deformation approaches the static value.
Figure 10 shows the relative deformation vs. time to be a sigmoid curve. The
implications of this curve remain to be exploited. It is apparent, however,
that the dynamic deformation of a dry mat is a complex function of pressure and
time. No simple rheological model that we have tried fits the data reasonably
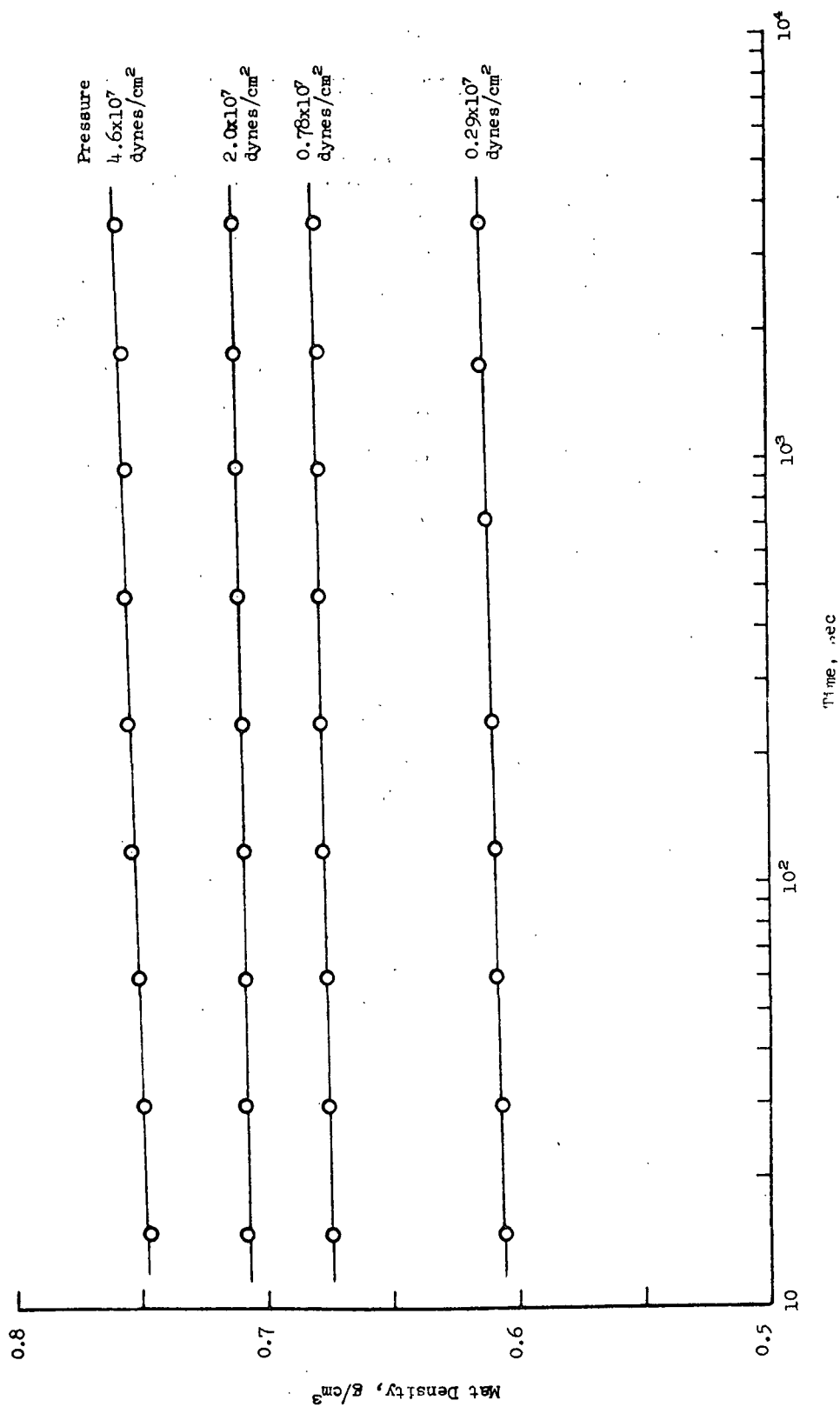well.

Figure 9. Creep of a Dacron Mat

TABLE IV

COMPARISON OF DYNAMIC AND STATIC COMPRESSION

| $t,$ sec $\times 10^3$	L, cm meas.	L, cm calc.	$\dfrac{L, \text{ calc.}}{L, \text{ meas.}}$	$\dfrac{L_0-L, \text{ cm}}{\text{meas.}}$	$\dfrac{L_0-L, \text{ cm}}{\text{calc.}}$	$\dfrac{\Delta L, \text{ meas.}}{\Delta L, \text{ calc.}}$
0	0.6826 = L_0					
5	0.6755	0.6554	0.972	0.0071	0.0272	0.260
6	0.6735	0.6498	0.965	0.0091	0.0328	0.269
7	0.6695	0.6429	0.961	0.0131	0.0397	0.330
8	0.6643	0.6326	0.953	0.0183	0.0500	0.366
9	0.6558	0.6114	0.932	0.0266	0.0712	0.373
10	0.6469	0.5931	0.917	0.0357	0.0895	0.399
11	0.6353	0.5722	0.902	0.0473	0.1104	0.427
12	0.6199	0.5588	0.900	0.0627	0.1238	0.506
13	0.6040	0.5489	0.910	0.0786	0.1337	0.588
14	0.5846	0.5259	0.900	0.0980	0.1567	0.625
15	0.5649	0.5050	0.895	0.1177	0.1776	0.662
16	0.5532	0.4973	0.897	0.1295	0.1853	0.699
17	0.5408	0.4912	0.906	0.1418	0.1914	0.727
18	0.5356	0.4877	0.909	0.1470	0.1949	0.755
19	0.5322	0.4856	0.912	0.1504	0.1970	0.765
20	0.5305	0.4853	0.914	0.1521	0.1973	0.771
21	0.5282	0.4828	0.918	0.1544	0.1998	0.773
22	0.5265	0.4804	0.913	0.1561	0.2022	0.773
23	0.5204	0.4746	0.911	0.1612	0.2080	0.778
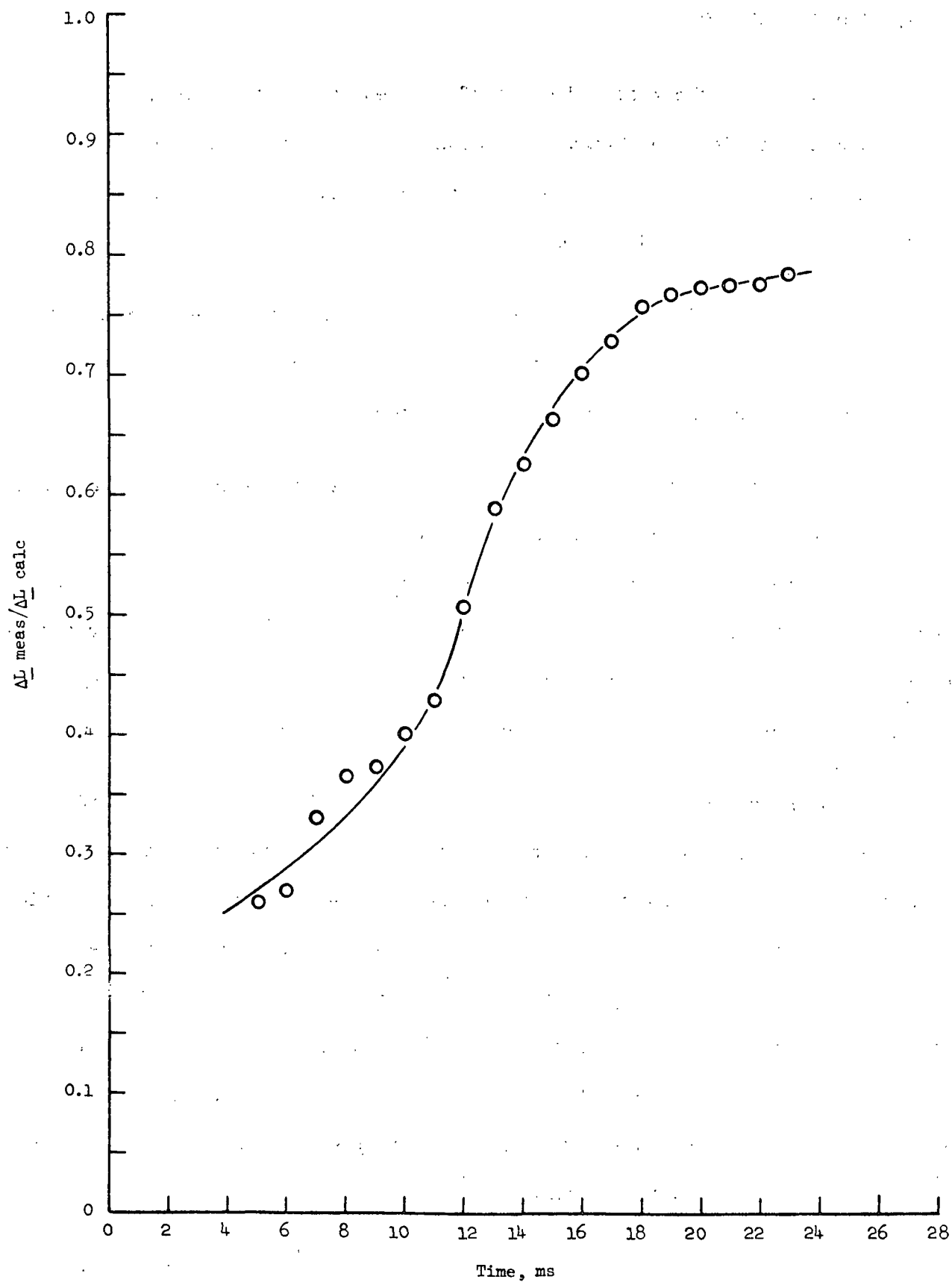
Figure 10. Comparison of Dynamic and Static Deformation

COMPRESSION OF WET MAT

Figure 11, the recorded chart of the wet compression test, reveals the generation and decay of hydraulic pressure. This constitutes the first direct experimental evidence to support the concept of compression-flow interaction which will soon be discussed.

The digitized data were processed in the same manner as in the dry compression test. The applied pressure was corrected for the piston inertia. Table V is a summary of the data in the early period of compression.

It is to be noted that the applied pressure data show, after an initial rise, a decrease between 6 and 12 ms. Experimentally, the pressure can only rise as the quick-acting air valve is turned open. Moreover, during those early times both the thickness and hydraulic pressure changes do not show any reversals. In view of these facts, the applied pressure data are smoothed as shown by the dashed segment of the corrected pressure curve in Fig. 12.

The measured hydraulic pressure is shown in Fig. 13 by the solid curve. The shape of the curve calls for some discussion. When a water-saturated mat is being compressed, the reduction of its volume must be balanced by the expression of water according to the principle of mass conservation. The instantaneous superficial velocity of flow out of the mat is approximately proportional to the rate of mat deformation. For slow flow through a uniform mat, the velocity is directly proportional to the hydraulic pressure. In the case of a nonuniform mat, we would expect that the curves of hydraulic pressure and deformation rate will at least show similar patterns.

The dashed curve in Fig. 13 represents the smoothed rate-of-deformation data on a vertical scale so chosen that the first peaks of the two curves have
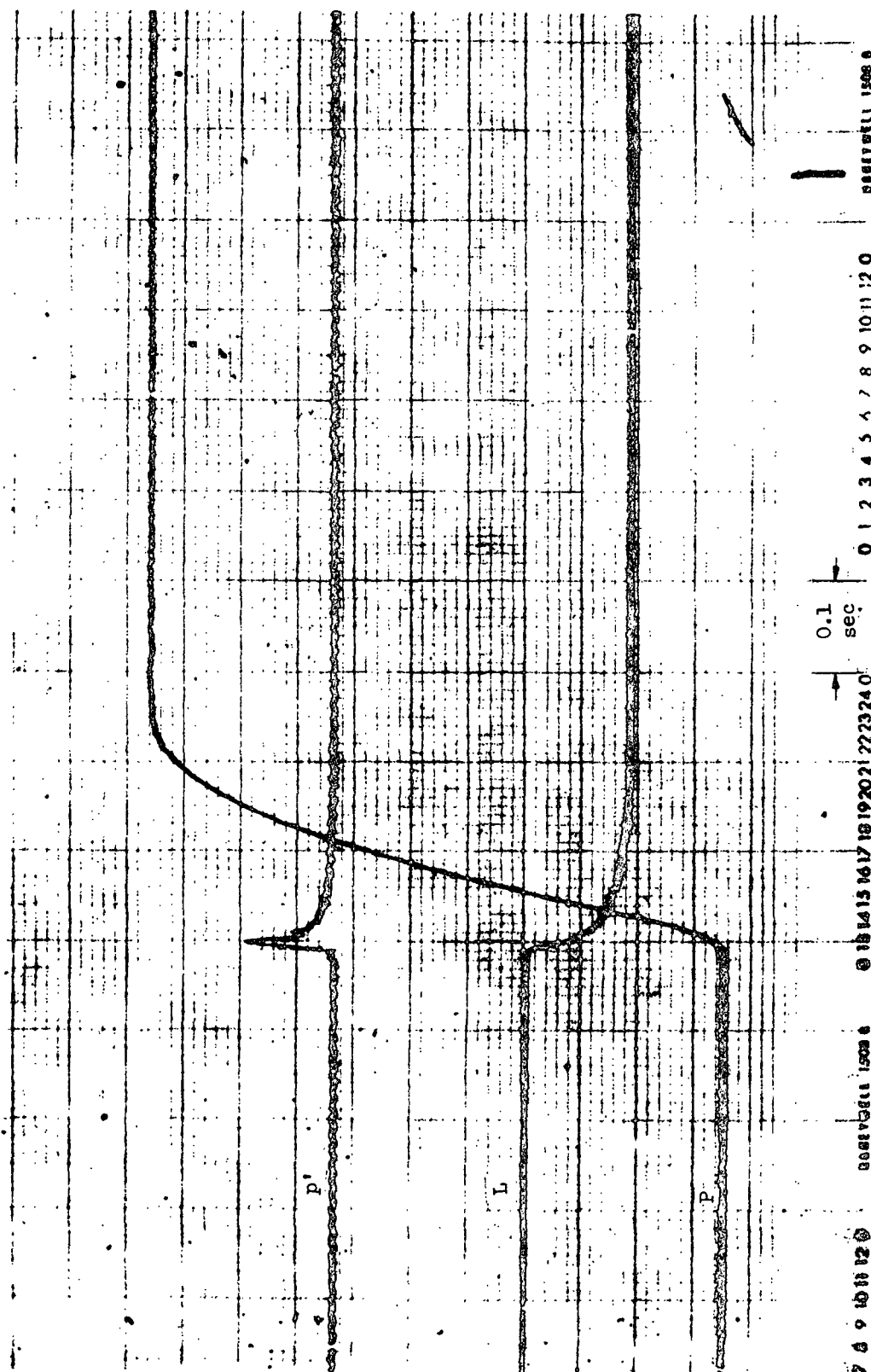
Figure 11. Wet Compression Chart

TABLE V

COMPRESSION OF WET MAT

| t, sec $\times 10^3$	P, dyne/cm^2 $\times 10^{-6}$		L, cm		p', dyne/cm^2 $\times 10^{-6}$	
	meas.	corr.	meas.	pred.	meas.	pred.
0	0.0688	0.0688	0.6222	0.6095	0	0
1.51	0.0886	0.0711	0.6218	0.6089	--	0.0209
3.03	0.115	0.0734	0.6215	0.6078	0.0245	0.0339
4.54	0.141	0.0758	0.6212	0.6064	0.0364	0.0411
6.06	0.147	0.0781	0.6208	0.6049	0.0552	0.0448
7.57	0.128	0.0804	0.6205	0.6034	0.0577	0.0463
9.09	0.102	0.0827	0.6201	0.6019	0.0577	0.0467
10.6	0.0843	0.0850	0.6197	0.6003	0.671	0.0463
12.1	0.0815	0.0873	0.6194	0.5989	0.0671	0.0457
13.6	0.0998	0.0902	0.6174	0.5974	--	0.0507
15.1	0.152	0.125	0.6132	0.5893	0.150	0.340
16.7	0.235	0.194	0.6054	0.5709	0.428	0.742
18.2	0.372	0.320	0.5930	0.5426	0.678	1.12
19.7	0.522	0.488	0.5804	0.5133	0.908	1.02
21.2	0.663	0.702	0.5646	0.4900	1.21	0.776
22.7	0.794	1.78	0.5457	0.4398	1.38	0.397
24.2	0.951	1.29	0.5309	0.4507	1.45	--
25.8	1.13	1.19	0.5121	0.4587	1.33	0.168
27.3	1.32	1.29	0.5104	0.4543	1.14	0.185
28.8	1.50	1.46	0.4937	0.4481	0.821	0.303
30.3	1.69	1.69	0.4890	0.4405	0.589	0.309
31.8	1.91	1.92	0.4831	0.4336	0.547	0.291
33.3	2.22	2.22	0.4752	0.4262	0.587	0.350
34.8	2.61	2.60	0.4693	0.4182	0.652	0.343
36.4	2.96	2.96	0.4630	0.4114	0.614	0.267
37.9	3.29	3.30	0.4563	0.4059	0.515	0.245
39.4	3.70	3.70	0.4515	0.4001	0.436	0.269
40.9	4.10	4.11	0.4468	0.3947	0.414	0.228
42.4	4.50	4.52	0.4424	0.3901	0.408	0.213
43.9	4.92	4.94	0.4391	0.3856	0.384	0.202
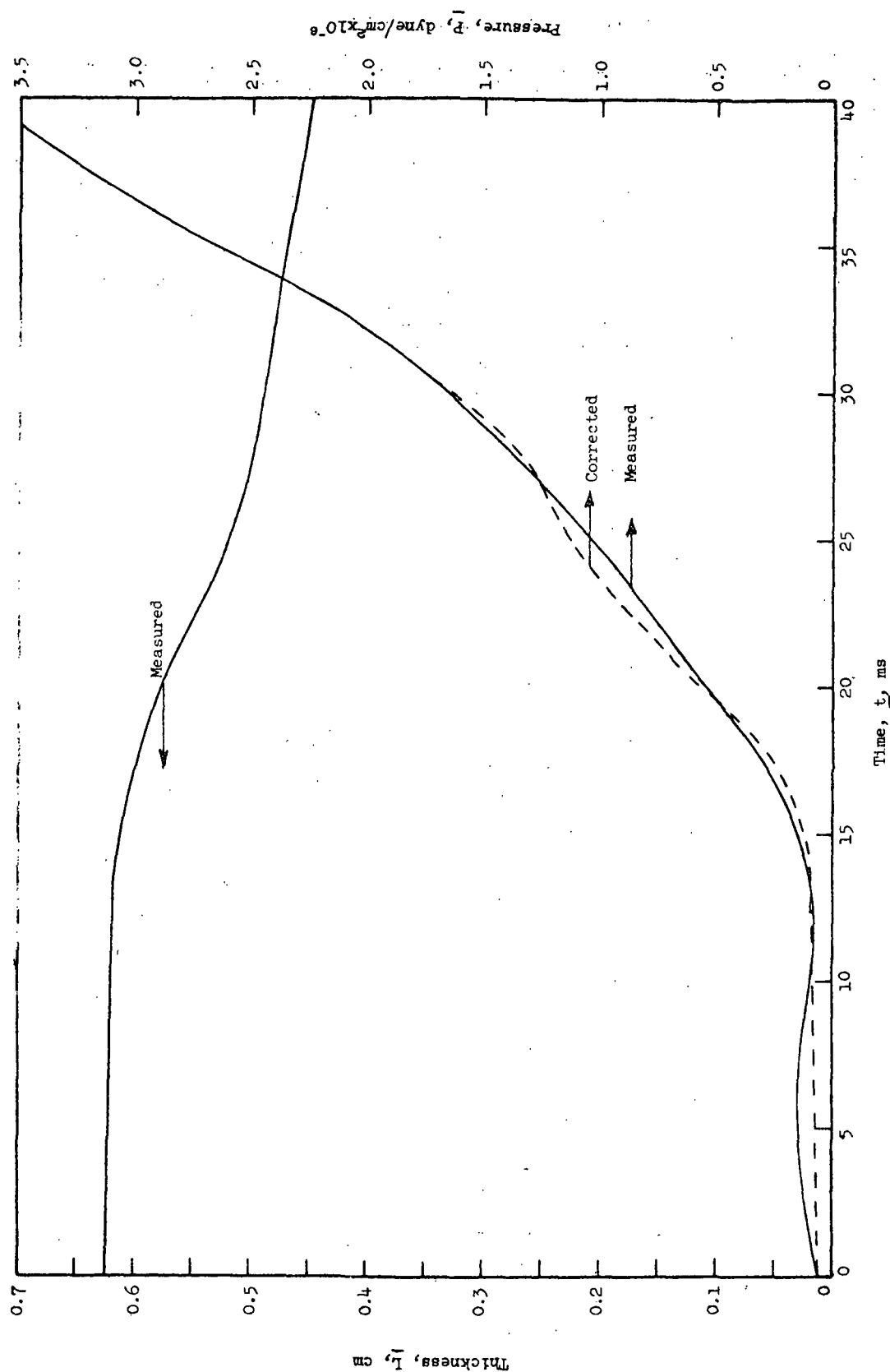
Figure 12. Pressure Correction for Wet Compression
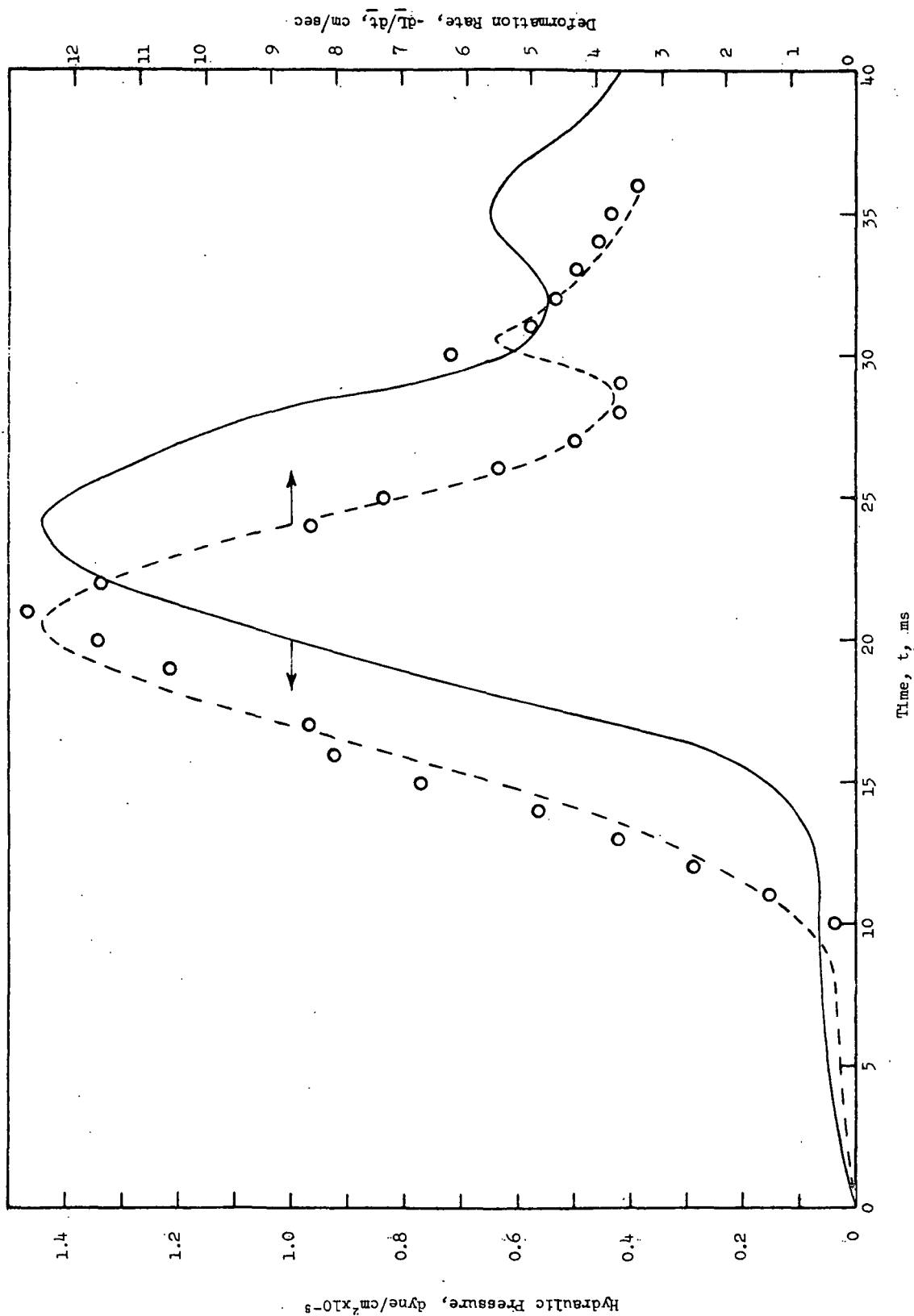
Figure 13.   Correspondence of Hydraulic Pressure with Rate of Deformation

the same height. It is seen that the two curves have largely the same pattern
of rise and fall, with a constant time difference. The hydraulic pressure lags
behind the deformation rate by 4 ms. Thus, if the deformation curve is shifted
forward, it will coincide with the main portion of the hydraulic pressure
curve between 15 and 30 ms.

This finding seems to imply that the deformation of the dacron mat is
also dependent on the rate of deformation, which is dictated by the applied
pressure schedule. The faster the pressure rise, the less effective may be the
compression at the same pressure.

At this point we digress for a moment to make a brief introduction of
the mathematical model for wet compression.

MATHEMATICAL MODELING OF WET COMPRESSION

The present model deals with the compression of a water-saturated mat
of solid fibers in a piston press such as the experimental apparatus. On a
macroscopic basis, the equations of continuity for water and fiber ($\underline{7}$) are related
by

$$\frac{\partial \varepsilon}{\partial t} = \frac{\partial U}{\partial z} = -\frac{\partial U'}{\partial z} \tag{6}$$

where a prime superscript denotes the fluid component.

If the forces required to produce acceleration in water and fiber can
be ignored, the pressure relation between the two components is

$$\frac{\partial p}{\partial z} = -\frac{\partial p'}{\partial z} \tag{7}$$

If the flow is slow, Darcy's law applies:

$$U' - \frac{\varepsilon}{1-\varepsilon} U = -\frac{1}{a} \frac{\partial p'}{\partial z} \tag{8}$$

or with the aid of the continuity equation,

$$U' = \varepsilon U'(o,t) - \frac{1-\varepsilon}{a} \frac{\partial p'}{\partial z} \tag{9}$$

where $a = \mu/K$.

Expressing porosity in terms of mat density, $\varepsilon = 1-c/\rho_f$, we obtain, by combining Equations (6), (7), and (9),

$$-\frac{\partial c}{\partial t} = U'(o,t) \frac{\partial c}{\partial z} - \frac{\partial}{\partial z} \left(\frac{c}{a} \frac{\partial p}{\partial z} \right) \tag{10}$$

which indicates the interaction of compression and flow.

To avoid the complication of a moving boundary, we may convert the equation of dynamic compression to a system of coordinates in which the independent variables are w and t, w being the cumulative mass of fiber per unit area:

$$w = \int_o^z c(z',t) \, dz', \quad o \leq w \leq W \tag{11}$$

The equation which results is

$$-\frac{\partial p}{\partial t} = \frac{c^2}{a} \left(\frac{\partial p}{\partial w} \right)^2 - c \left(\frac{\partial p}{\partial c} \right) \frac{\partial}{\partial w} \left(\frac{c^2}{a} \frac{\partial p}{\partial w} \right) \tag{12}$$

The experimental conditions are that the boundary at $z = o$ is impermeable to either component, $U'(o,t) = o$, and that the mat is confined at $z = L$, by a piston which offers no resistance to fluid flow. Thus, the initial condition is that $c(z,o)$ or $p(z,o)$ have assigned values, and the boundary conditions turn out to be

$$\left(\frac{\partial p}{\partial z} \right)_{z=o} = o \tag{13}$$

and

$$p(L,t) = P(t) \tag{14}$$

The required information is compressibility, $\underline{c}(\underline{p},\underline{t})$, and permeability, $\underline{K}(\varepsilon,\underline{S}_v)$, of the mat. At present we assume that the experimentally determined compressibility function in a static test and permeability function in a steady state are applicable to dynamic compression. Then, given an applied pressure schedule, $\underline{P}(\underline{t})$, the model will predict $\underline{p}(\underline{w},\underline{t})$ and, in particular, the mat thickness, $\underline{L}(\underline{t})$, as well as the fluid pressure, $\underline{p}'(o,\underline{t})$, at the impermeable boundary. The last two predictions may be directly compared with the data. The numerical treatment of the model is discussed in the appendix.

COMPARISON OF PREDICTIONS WITH EXPERIMENT

The results of prediction for the wet compression test are tabulated in Table V. The predicted thickness is 2-13% smaller than the measured values. This discrepancy arises mainly from the use of the static compressibility function. To improve the predictions we must seek an appropriate dynamic function, $\underline{c}(\underline{p},\underline{t})$ for use in the model.

Of much more interest is a comparison of the predicted and measured hydraulic pressure which is an essential feature of flow-influenced wet pressing. Such a comparison is shown in Fig. 14. The discussion follows:

1. The slow rise — The predictions in this beginning period are based on the smoothed pressure rise. They agree quite well with the data. It should be mentioned that when the digitized data of applied pressure were used, the model predicted a rise of hydraulic pressure in the first 6 ms and a fall to a vacuum in the next 6 ms. The generation of a vacuum would indicate a rapid expansion of the mat in contradiction to the experimental facts, as previously pointed out. The predicted vacuum arises
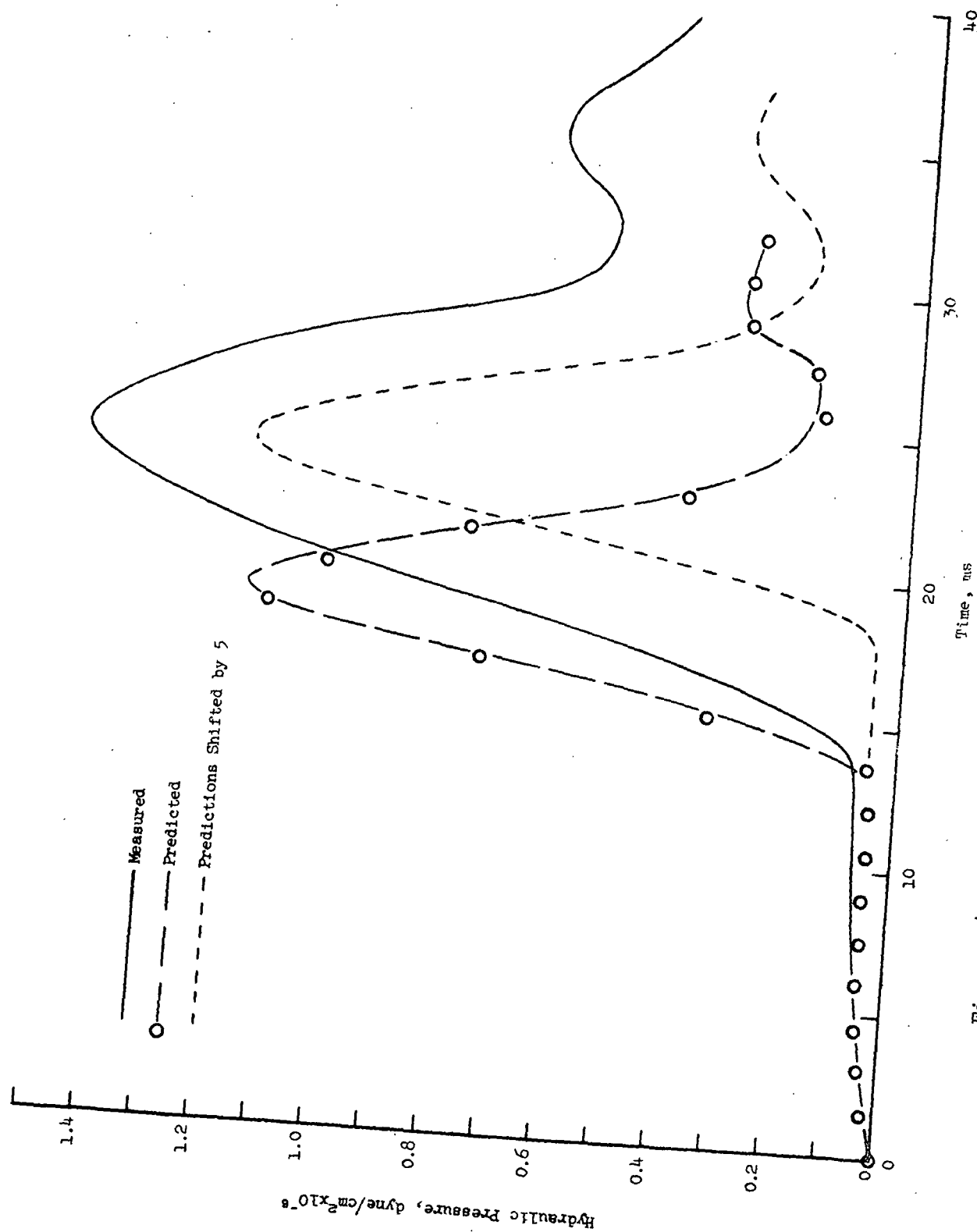
Figure 14. Comparison of Predicted and Measured Hydraulic Pressure

from a fall of the applied pressure. The predictions are
further exaggerated by the assumption of equilibrium compressibility.

2. The first hump — In the next period of a fast rise to the
    first peak and a fast drop to the first valley, the two curves
    look very similar. Again, the experimental curve lags behind
    the predictions. By shifting the predicted curve along the
    time axis until the two peaks fall on the same vertical line,
    the correspondence of the two curves is more clearly demonstrated.
    The time lag is about 5 ms. This lag may be attributed largely
    to the use of the static compressibility in the model, and is
    probably related to the previous finding in connection with the
    rate of deformation. The predicted peak is about 30% lower than
    the measured value. This discrepancy may be partly due to the errors
    accumulated in the model up to that time. The model is very
    sensitive to the details of the applied pressure schedule.

3. The second hump — The predicted second hump corresponds satis-
    factorily to the measured one on the shifted time scale, but the
    magnitude of discrepancy is getting much larger. Further comparison
    and interpretation do not appear to be justified until the matter
    of dynamic compressibility is clarified.

In conclusion, wet pressing of a fiber mat involves the interaction of
mechanical compression and water flow. This interaction is experimentally demon-
strated by the generation and decay of hydraulic pressure, and can be simulated
by the proposed mathematical model. A reliable account for the compression-flow
phase of wet pressing requires a knowledge of the load-deformation-time behavior

of the fiber structure. Even without such knowledge, the use of the model aided

by some controlled experiments is still an advantageous way to investigate the

relative effects of the parameters important in pressing.

NOMENCLATURE

a = viscous resistance, dynes $\times$ sec/cm^2

c = mat density, g/cm^3

c_o = compressibility parameter, g/cm^3

k = Kozeny factor, dimensionless

K = permeability, cm^2

L = mat thickness, cm

M = compressibility parameter, (g/cm^3)/(dyne/cm^2)$^{\underline{N}}$

M_1 and M_2 = creep parameters, (g/cm^3)/(dyne/cm^2)$^{\underline{N}}$

ms = milliseconds

p = compacting pressure, dyne/cm^2

p' = fluid pressure, dyne/cm^2

P = applied pressure, dyne/cm^2

S_v = specific surface, 1/cm

t = time, second

U = fiber velocity, cm/sec

U' = water velocity, cm/sec

w = mass coordinate, g/cm^2

W = basis weight, g/cm^2

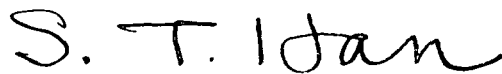z = thickness coordinate, cm

Greek Symbols:

Δ = finite difference

ε = porosity, dimensionless

μ = viscosity, g/(cm)(sec)

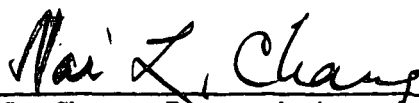ρ_f = density of fiber, g/cm^3

LITERATURE CITED

1. Ingmanson, W. L., and Whitney, R. P., Tappi 37(11):523(1954).

2. Kurath, S. F., etc. The relation of mechanical properties of single fibers to the mechanical behavior of fiber networks. Report Four, Project 2210, The Institute of Paper Chemistry, Appleton, WI, Dec. 12, 1961.

3. Han, S. T., Pulp Paper Mag. Can. 70(9):T134(1969).

   Wilder, H. D. The compression creep properties of wet pulp mats. Doctoral Dissertation. The Institute of Paper Chemistry, Appleton, WI, 1959; Tappi 43(8):715(1960).

5. Wahlstrom, P. B. Our present understanding of the fundamentals of pressing. 1968 International Symposium on Water Removal at the Presses and Dryers, Mont Gabriel P.Z., Canada, Oct., 1968.

6. Ingmanson, W. L., and Andrews, B. D., Tappi 46(3):150(1963).

7. Nelson, R. W., Tappi 47(12):752(1964).

8. Davies, C. N., Proc. Inst. Mech. Engrs. (London) 1B:185(1952).

9. Emmons, H. W., Tappi 48(12):679(1965).

10. Carnahan, B., Luther, H. A., and Wilkes, J. O., Applied numerical methods. Chap. 7. New York, Wiley, 1969.

11. Fox, L., ed. Numerical solution of ordinary and partial differential equations. Chaps. 19 and 20. Addison-Wesley, 1962.

12. Fröberg, C.-E. Introduction to numerical analysis. 2nd Edition. Chap. 15. Addison-Wesley, 1969.

13. Carroll, C. W. Unpublished work. The Institute of Paper Chemistry, 1965.

THE INSTITUTE OF PAPER CHEMISTRY

S. T. Han, Senior Research Associate

N. L. Chang, Research Associate
Division of Materials
Engineering & Processes

APPENDIX I

COMPRESSION OF A SATURATED MAT: MATHEMATICAL MODELS

In the outline which follows, we present a simplified but realistic description of the effects of an applied stress on a saturated mat, considered as an interacting system (a liquid and a porous solid). The model involves a stratified structure — properties depend upon only one spatial variable. Although we do not dismiss other possibilities as irrelevant, the model (a) neglects time-dependent phenomena in mat compressibility, (b) omits the consequences of inertia in the mat and in the fluid, and (c) utilizes a linear relation connecting fluid pressure gradient and flow rate. These limitations lead to a formulation of the problem which consists of a nonlinear partial differential equation with easily stated initial and boundary conditions, and is amenable to numerical solution.

In the choice of method, and of computational procedure, we have attempted to anticipate subsequent changes in the hypotheses, and to provide enough flexibility where it is likely to be needed.

We assume that the solids concentration $\underline{c}(\underline{z},\underline{t})$ and the stress in the solid phase $\underline{p}(\underline{z},\underline{t})$ are directly connected, as in

$$c = c_o + Mp^N.$$

For use in the numerical solutions, the parameters $\underline{c}_o$, $\underline{M}$, and $\underline{N}$ were determined by a least-squares adjustment, from measurements on the mat to be used in the pressure-impulse experiment. Omission of the parameter $\underline{c}_o$ gave a less satisfactory correlation.

Our procedure, however, is in no way limited to this empirical relationship, and will admit any appropriate connection, even if it is available only in terms of tabular information.

As will be noted presently, we have also considered the possibility that the local and current value of c might depend on the history of the local solid-phase stress p; but in the absence of experimental information we have not attempted to develop a numerical treatment.

The theory will permit an approximate account of effects due to inertia in the fluid and in the solid phases, should this become necessary.

The model, as elaborated, assumes that the fluid pressure gradient and the flow rates are connected as in

$$U'(z,t) - [\epsilon/(1 - \epsilon)] U(z,t) = - a^{-1} (\partial p'/\partial z) , \qquad (15)$$

where p' is the fluid pressure, and a is a function of the porosity and characteristics of the solid component of the system. The present assumption of essentially percolative flow is not a necessary limitation of the theory, but is considered to be adequate.

When inertial effects within the system are omitted, the description of the linked solid- and liquid-phase system, as shown by Nelson ([7]) and Emmons ([9]), is contained in such equations as

$$- (\partial c/\partial t) = U'(0,t) (\partial c/\partial z) - (\partial/\partial z)[c/a^{-1}(\partial p/\partial z)] . \qquad (16)$$

The independent variables are z and t, where z is the spatial coordinate, and the system extends from $z = 0$ to $z = L$; and $U'(0,t)$ is the superficial velocity of the fluid at $z = 0$.

For the present purpose, the basis weight is assumed to be constant, but the applied pressure schedule will decrease the mat thickness L. To avoid the complication of a moving boundary, we may convert to a system of coordinates in which the independent variables are w and t, where w is the cumulative mass:

$$w = \int_0^z c(z',t)\, dz' \, . \tag{17}$$

The equation which results is

$$- (\partial c / \partial t) = c^2\, a^{-1}\ (\partial p / \partial w)\ (\partial c / \partial w)$$
$$- c\ (\partial / \partial w)\ [c^2\, a^{-1}\ (\partial p / \partial w)]\ . \tag{18}$$

Scrutiny of the argument leading to Equation (18) shows that it applies not only to the situation represented by Equation (1) or an alternative connection, but also when $\underline{c}$ is the outcome of present and previous values of the local solid-phase stress; an observation which includes (but is not limited to) a solids concentration which can be calculated as an integral transform of the record of the local stress as a function of $\underline{t}$.

In the cases which we have reduced to computational procedures, however, $\underline{c}$ is a point function which depends only on the local and current value of $\underline{p}$. For these, we arrange Equation (18) in the form

$$- (\partial p / \partial t) = c^2\, a^{-1}\ (\partial p / \partial w)^2$$
$$- c\ \zeta^{-1}\ (\partial / \partial w)\ [c^2\, a^{-1}\ (\partial p / \partial w)]\ , \tag{19}$$

where

$$\zeta\ (p) = (dc/dp)\ . \tag{20}$$

In Equations (18) and (19), the range of $\underline{w}$ is fixed:

$$0 \leqq w \leqq W = \int_0^L c(z',t)\, dz' \, . \tag{21}$$

The experimental conditions are that the boundary at $\underline{z} = 0$ is impermeable to either component, so that, in particular, $\underline{U}'(0,\underline{t}) = 0$; and that the mat is confined at $\underline{z} = \underline{L}$ by a piston which offers negligible resistance to fluid flow. Thus, the initial condition is that $\underline{c}(\underline{z},0)$ or $\underline{p}(\underline{z},0)$ have assigned values, and the

boundary conditions turn out to be that, for $\underline{z}$ = 0 and all values of $\underline{t}$,

$$(\partial p / \partial z) = 0 , \qquad (22)$$

and

$$p(L,t) = P(t) = \text{applied load per unit area.} \qquad (23)$$

We have completed and tested numerical treatments of this problem under three different assumptions as to the form of the function $\underline{a}$. In the first of these, the chosen form is

$$a = \gamma\mu \, S_v^2 \, (1 - \varepsilon)^{3/2} \, [1 + b \, (1 - \varepsilon)^3] , \qquad (24)$$

in which we have inserted the numerical values recommended by Ingmanson ($\underline{6}$) for use in Davies' correlation ($\underline{8}$),

$$k = \gamma\varepsilon^3 \, (1 - \varepsilon)^{-1/2} \, [1 + b \, (1 - \varepsilon)^3] . \qquad (25)$$

The details appear in Appendix II.

In the second numerical treatment, we have taken

$$a = \mu \, S_v^2 \, [(1 - \varepsilon)^2/\varepsilon^3] \, \{5.0 + \exp[13.5 \, (\varepsilon - 0.8)]\} , \qquad (26)$$

a form proposed by Carroll ($\underline{13}$), with the further assumption that

$$S_v = S_{v,0} \, [1 - (\varepsilon_0 - \varepsilon)] . \qquad (27)$$

where ε_0 = 0.88. In the notation of Appendix II, we now have

$$\theta = R \, \varepsilon^3 \, [1 - (\varepsilon_0 - \varepsilon)]^{-2} \, \{5.0 + \exp[13.5 \, (\varepsilon - 0.8)]\}^{-1} , \qquad (28)$$

with $\underline{R} = \rho_f^2/(\mu S_{v,0}^2)$, and the formula for ξ is unchanged. The expressions for the first and second derivatives of θ become quite complicated. The program (CN2:3258/8=880A) also embodies the Crank-Nicolson method and differs from that

reported in Appendix II (CN1:3258/2=874A) only in the systematic modification of a few details.

In the third numerical treatment, the flow resistance is accounted for in terms of (separately) measured values of $\underline{a}$ as a function of ε. We represent θ as a function of $\underline{p}$ by a least-squares adjustment of an empirical formula, where, again in the notation of Appendix II,

$$\theta = \rho_f^2 \, (1 - \varepsilon)^2 / a \, , \tag{29}$$

and $\underline{p}$ is calculated from

$$c_0 + Mp^N = \rho_f \, (1 - \varepsilon) \, . \tag{30}$$

The resulting program (CN3:3258/9=881A) applies the Crank-Nicolson method and differs from the preceding examples (CN1 and CN2) only in details.

Richard W. Nelson

APPENDIX II

COMPRESSION OF A SATURATED MAT: NUMERICAL SOLUTIONS

We consider numerical methods and program design for the solution of a nonlinear partial differential equation, having a general resemblance to the parabolic type of equation familiar in the formulation of heat-conduction problems (10-12). There is only one spatial independent variable. The equation and auxiliary conditions, which are to be discussed, arise in the description of fluid flow through a deformable porous medium, under certain simplifying assumptions. Two possibilities were selected and programmed: the 'explicit' method, which has the advantage of simplicity and the disadvantage of an inconvenient time step limitation; and an 'implicit' method (the Crank-Nicolson procedure). The latter introduces a novelty, in that one must solve a system of nonlinear equations (of special form) in completing each time step.

The solution is defined by the equation

$$u_t = A(u) (u_x)^2 + B(u) u_{xx} , \qquad (31)$$

together with a given initial state

$$u(x,0+) = f(x) , \qquad (32)$$

and the boundary conditions

$$u_x(0+, t) = 0 \qquad \text{and} \qquad u(X-, t) = g(t) . \qquad (33)$$

For convenience, the notation uses subscripts to indicate the construction of partial derivatives; thus u_t means $(\partial u/\partial t)$, and u_{xx} means $(\partial^2 u/\partial x^2)$.

In the application at hand, $\underline{u}$ is the stress in the solid portion of the system, and the independent variable $\underline{x}$ is the cumulative mass per unit area (in the solid portion).   Then

$$A(u) = \xi\theta' - \theta , \tag{34}$$

$$B(u) = \xi\theta , \tag{35}$$

where

$$\xi = (c_0 + M u^N)/(N M u^{N-1}) , \tag{36}$$

and

$$\theta = [\rho_f^2(1 - \varepsilon)^{1/2}]/\{\gamma [1 + b (1 - \varepsilon)^3]\} , \tag{37}$$

in which

$$1 - \varepsilon = (c_0 + M u^N)/\rho_f . \tag{38}$$

EXPLICIT METHOD (EXPL:3258/1=873A)

With the space index $\underline{p}$ taking on values from 1 through $\underline{n}$, the transcription of the equation becomes

$$v(1, q+1) = \lambda B[v(1, q)] [2 v(2, q) - 2 v(1, q)] , \tag{39}$$

and, for $2 \leq \underline{p} \leq \underline{n}-1$,

$$v(p, q+1) = (\lambda/4) A[v(p, q)] [v(p+1, q) - v(p-1, q)]^2$$

$$+ \lambda B[v(p, q)] [v(p+1, q) - 2 v(p, q) + v(p-1, q)] , \tag{40}$$

while

$$v(n, q+1) = g(t_{q+1}) . \tag{41}$$

The time step parameter is $\lambda = (\Delta\underline{t})/(\Delta\underline{x})^2$; and the construction of Equations (39) and (41) accounts for the boundary conditions.

Program 873A mechanizes the process represented by Equations (39), (40), and (41). Tests confirm the presence of the expected and inherent time step limitation, the effect of which is to set a maximum value for the product λB. Further, one may question the ability of this method to respond correctly to rapid changes in $g(t)$, since the procedure imports a dubious propagation-time effect, which is not in harmony with the structure of Equation (1).

CRANK-NICOLSON METHOD (CN1:3258/2=874A)

The Crank-Nicolson method introduces central-difference approximations for the space derivatives. We have chosen the following as appropriate to the generalization required here:

u_t is replaced by $[v(p, q+1) - v(p, q)]/(\Delta t)$, as usual; $\qquad$ (42)

$A(u) (u_x)^2$ is replaced by

$$(1/2) A[v(p, q+1)] \{[v(p+1, q+1) - v(p-1, q+1)]/(2\Delta x)\}^2$$

$$+ (1/2) A[v(p, q)] \{[v(p+1, q) - v(p-1, q)]/(2\Delta x)\}^2 ; \qquad (43)$$

$B(u) u_{xx}$ is replaced by

$$(1/2) B[v(p, q+1)] [v(p+1, q+1) - 2 v(p, q+1) + v(p-1, q+1)]/(\Delta x)^2$$

$$+ (1/2) B[v(p, q)] [v(p+1, q) - 2 v(p, q) + v(p-1, q)]/(\Delta x)^2 . \qquad (44)$$

With cases distinguished as before, the difference equation becomes

$$- \{2 + 2 \lambda B[v(1, q+1)]\} v(1, q+1) + 2 \lambda B[v(1, q+1)] v(2, q+1) =$$

$$- \{2 - 2 \lambda B[v(1, q)]\} v(1, q) - 2 \lambda B[v(1, q)] v(2, q) , \qquad (45)$$

and, for $2 \leq p \leq n-1$,

$$\lambda B[v(p,\ q+1)]\ v(p-1,\ q+1) - \{2 + 2\ \lambda B[v(p,\ q+1)]\}\ v(p,\ q+1)$$

$$+\ \lambda B[v(p,\ q+1)]\ v(p+1,\ q+1)$$

$$+\ (1/4)\ \lambda A[v(p,\ q+1)]\ [v(p+1,\ q+1) - v(p-1,\ q+1)]^2 =$$

$$-\ \lambda B[v(p,\ q)]\ v(p-1,\ q) - \{2 - 2\ \lambda B[v(p,\ q)]\}\ v(p,\ q)$$

$$-\ \lambda B[v(p,\ q)]\ v(p+1,\ q)$$

$$-\ (1/4)\ \lambda A[v(p,\ q)]\ [v(p+1,\ q) - v(p-1,\ q)]^2\ , \tag{46}$$

while

$$v(n,\ q+1) = g(t_{q+1})\ . \tag{47}$$

We solve this system of simultaneous equations (once per time step) by an iterative method, computing the correction at each stage of iteration from a linearized version of the system of equations. The initial approximation is always taken to be the current state of the system [except for the introduction of the updated value of $\underline{v}(\underline{n},\ q+1)$, as given by Equation (47)]. The linearized version has the familiar form of a tridiagonal set of linear equations, and to this we apply a convenient recursive procedure [Reference (10), p. 441-2]. A listing of the subprogram for this procedure (TRI:3258/3=875A) appears separately, following the other programs.

Let $\underline{w}(\underline{p},\ q+1;\ \underline{j})$ be the approximate solution, at stage $\underline{j}$ of the process just described. In this notation, $\underline{w}(\underline{p},\ q+1;\ 0) = \underline{v}(\underline{p},\ q)$ for $1 \leqq \underline{p} \leqq \underline{n}-1$, $\underline{w}(\underline{n},\ q+1;\ \underline{j}) = \underline{g}(t_{q+1})$ for $0 \leqq \underline{j}$; and with the abbreviation $\delta w_{\underline{p}} = \underline{w}(\underline{p},\ q+1;\ \underline{j}+1) - \underline{w}(\underline{p},\ q+1;\ \underline{j})$ the linearized version is

$$G_1\ \delta w_1 + H_1\ \delta w_2 = K_1\ , \tag{48}$$

$$F_r\ \delta w_{r-1} + G_r\ \delta w_r + H_r\ \delta w_{r+1} = K_r\ ,\quad 2 \leqq r \leqq n-2\ , \tag{49}$$

$$F_{n-1} \, \delta w_{n-2} + G_{n-1} \, \delta w_{n-1} = K_{n-1} \, . \tag{50}$$

where

$$G_1 = -2 - 2 \lambda B[w(1, q+1; j)]$$

$$- 2 \lambda[w(1, q+1; j) - w(2, q+1; j)] \, B'[w(1, q+1; j)] \, , \tag{51}$$

$$H_1 = 2 \lambda B[w(1, q+1; j)] \, , \tag{52}$$

$$K_1 = -2 \lambda B[w(1, q+1; j)] \, w(2, q+1; j)$$

$$+ \{2 + 2 \lambda B[w(1, q+1; j)]\} \, w(1, q+1; j)$$

$$- 2 \lambda B[v(1, q)] \, v(2, q) - \{2 - 2 \lambda B[v(1, q)]\} \, v(1, q) \, , \tag{53}$$

$$F_r = \lambda B[w(r, q+1; j)]$$

$$- (1/2) \lambda A[w(r, q+1; j)] \, [w(r+1, q+1; j) - w(r-1, q+1; j)] \, , \tag{54}$$

$$G_r = -2 - 2 \lambda B[w(r, q+1; j)]$$

$$+ \lambda[w(r+1, q+1; j) - 2 w(r, q+1; j) + w(r-1, q+1; j)] \, B'[w(r, q+1; j)]$$

$$+ (1/4) \lambda[w(r+1, q+1; j) - w(r-1, q+1; j)]^2 \, A'[w(r, q+1; j)] \, , \tag{55}$$

$$H_r = \lambda B[w(r, q+1; j)]$$

$$+ (1/2) \lambda A[w(r, q+1; j)] \, [w(r+1, q+1; j) - w(r-1, q+1; j)] \, , \tag{56}$$

$$K_r = - \lambda B[w(r, q+1; j)] \, [w(r+1, q+1; j) + w(r-1, q+1; j)]$$

$$+ \{2 + 2 \lambda B[w(r, q+1; j)]\} \, w(r, q+1; j)$$

$$- (1/4) \lambda A[w(r, q+1; j)] \, [w(r+1, q+1; j) - w(r-1, q+1; j)]^2$$

$$- \lambda B[v(r, q)] \, [v(r+1, q) + v(r-1, q)]$$

$$- \{2 - 2 \lambda B[v(r, q)]\} \, v(r, q)$$

$$- (1/4) \lambda A[v(r, q)] \, [v(r+1, q) - v(r-1, q)]^2 \, . \tag{57}$$

As it happens, Equations (54), (55), and (57) also give the coefficients
which appear in the last equation of the linearized set, Equation (50), when one
takes $\underline{r} = \underline{n}-1$.

In the percolative flow problem, we have

$$A(u) = \xi\theta' - \theta , \qquad (58)$$

$$B(u) = \xi\theta , \qquad (59)$$

$$A'(u) = \xi\theta'' + (\xi' - 1) \theta' , \qquad (60)$$

$$B'(u) = \xi\theta' + \xi'\theta , \qquad (61)$$

with the definitions of ξ and θ given in Equations (36) and (37), respectively.
Formulas for ξ', θ', and θ'' appear separately, on the following page.

TESTS

The programs (EXPL and CN1) have been compared under circumstances accept-
able to both, with satisfactory agreement. The latter (CN1) has the stability which
would be expected; it has been noted, however, that very rapid variation in $\underline{g}(\underline{t})$
can lead to failure of convergence in the iterative cycle. Although the problem
has not been encountered often enough to justify immediate attention, it should be
possible to remove or defer this complication through such improvements in the
design as a more tractable initial state for each time step, and devices to diminish
oscillations.

Further comparisons (CN1, with progressively larger values for the time
step parameter) have confirmed the capacity of this approach to lessen the volume
of calculation required in tracing the evolution of the system.

$$\xi' = 1 - (c_0 + M u^N)(N - 1)/(N M u^N), \tag{62}$$

$$\theta' = (M N \theta/\rho_f)\{(1/2)/(1 - \epsilon) - 3 b (1 - \epsilon)^2/[1 + b (1 - \epsilon)^3]\} u^{N-1}, \tag{63}$$

$$\theta'' = [M N (N - 1) \theta/\rho_f]\{(1/2)/(1 - \epsilon) - 3 b (1 - \epsilon)^2/[1 + b (1 - \epsilon)^3]\} u^{N-2}$$
$$+ (M N/\rho_f)^2 \theta \{- (1/4)/(1 - \epsilon)^2 - 9 b (1 - \epsilon)/[1 + b (1 - \epsilon)^3]$$
$$+ 18 b^2 (1 - \epsilon)^4/[1 + b (1 - \epsilon)^3]^2\} u^{2N-2}. \tag{64}$$

PROGRAM LISTINGS

       (1)   Program for the Explicit Method (EXPL:3258/1=873A)

       (2)   Program for the Crank-Nicolson Method (CN1:3258/2=874A)

       (3)   Subprogram for Solution of Tridiagonal System

           (TRI:3258/3=875A)

                             Richard W. Nelson

```
C           PROJECT 3258    R W NELSON    20 NOVEMBER 1974
C           DEWATERING PROBLEM    EXPLICIT METHOD (EXPL 3258/1=873A)
C                 PART A, PRELIMINARIES
      DIMENSION POST(100), STEP(100)
      COMMON T, P, NR
      READ (5,302)  L, IND, MAX
      READ (5,301)  PREV, ALPHA, COEFF
      READ (5,301)  PARAM, QN, B, CN
      READ (5,301)  CU, RHO, QMT
      WRITE (6,310)
      WRITE (6,312)  L, IND, MAX
      WRITE (6,311)  PREV, ALPHA, COEFF
      WRITE (6,311)  PARAM, QN, B, CN
      WRITE (6,311)  CU, RHO, QMT
      WRITE (6,306)
      NR = 1
      CALL FNCT
      NR = 2
      WRITE (6,315)
      LP1 = L + 1
      QNM1 = QN - 1.0
      KTR = 0
      MARK = 0
      DO 5  I = 1, LP1
    5 STEP(I) = PREV
      TEMP = L
      SAVE = QMT / TEMP
      DELT = SAVE * SAVE * ALPHA
      T = DELT
      CALL FNCT
      POST(LP1) = P
      WRITE (6,335)
      TIME = 0.0
      TEMP = 0.0
      DO 3  I = 2, L
    3 TEMP = TEMP + 1.0 / (CN + CU * (STEP(I) ** QN))
      TEMP = TEMP + 0.5 / (CN + CU * (STEP(1) ** QN))
    1       + 0.5 / (CN + CU * (STEP(LP1) ** QN))
      SAVE = L
      TEMP = TEMP * QMT / SAVE
      STORE = TEMP - QMT / RHO
      WRITE (6,325)  MARK, TIME, TEMP, STORE
      WRITE (6,306)
      DO 4  I = 1, LP1
    4 WRITE (6,325)  I, STEP(I)
      WRITE (6,315)
      WRITE (6,336)
C                 PART B, CYCLE
  211 G = STEP(1)
      H = STEP(2)
      TEMP = ALOG(G)
      U = EXP(QN * TEMP)
      V = EXP(QNM1 * TEMP)
      REGA = CN + CU * U
      REGB = CU * QN * V
      FRACT = REGA / RHO
```

```
      TEMP = FRACT * FRACT
      SAVE = TEMP * FRACT
      STORE = 1.0 + B * SAVE
      QF = COEFF * SQRT(FRACT) / STORE
      QK = REGA / REGB
      S = ALPHA * QK * QH
      POST(1) = 2.0 * S * (H - G) + G
      DO 201 I = 2, L
      F = STEP(I-1)
      G = STEP(I)
      H = STEP(I+1)
      TEMP = ALOG(G)
      U = EXP(QN * TEMP)
      V = EXP(QNM1 * TEMP)
      REGA = CN + CU * U
      REGB = CU * QN * V
      FRACT = REGA / RHO
      TEMP = FRACT * FRACT
      SAVE = TEMP * FRACT
      STORE = 1.0 + B * SAVE
      QH = COEFF * SQRT(FRACT) / STORE
      QK = REGA / REGB
      QHP = PARAM * QH * (0.5 / FRACT - 3.0 * B * TEMP / STORE) * V
      R = ALPHA * (QK * QHP - QH) / 4.0
      S = ALPHA * QK * QH
      TEMP = H - F
      SAVE = F - 2.0 * G + H
  201 POST(I) = R * TEMP * TEMP + S * SAVE + G
C              PART C, OUTPUT
      KTR = KTR + 1
      IF (KTR - IND)  220, 221, 221
  221 KTR = 0
      MARK = MARK + IND
      TEMP = MARK
      TIME = TEMP * DELT
      TEMP = 0.0
      DO 701 I = 2, L
  701 TEMP = TEMP + 1.0 / (CN + CU * (POST(I) ** QN))
      TEMP = TEMP + 0.5 / (CN + CU * (POST(1) ** QN))
     1      + 0.5 / (CN + CU * (POST(LP1) ** QN))
      SAVE = L
      TEMP = TEMP * QMT / SAVE
      STORE = TEMP - QMT / RHO
      WRITE (6,325)  MARK, TIME, TEMP, STORE
      WRITE (6,306)
      DO 251  I = 1, LP1
      STEP(I) = POST(I)
  251 WRITE (6,325)  I, POST(I)
      WRITE (6,315)
      IF (MARK - MAX)  253, 407, 407
  407 CALL EXIT
  220 DO 202  I = 1, LP1
  202 STEP(I) = POST(I)
  253 TEMP = KTR + MARK + 1
      T = TEMP * DELT
      CALL FNCT
```

```
      POST(LP1) = P
      GO TO 211
C                  PART D, I/O ARRANGEMENTS
  301 FORMAT (4E15.7)
  302 FORMAT (3I5)
  306 FORMAT (1H )
  310 FORMAT (1H , 4X, 'DATA FOR MAIN PROGRAM', /)
  311 FORMAT (1H , 4X, E15.7, 5X, E15.7, 5X, E15.7, 5X, E15.7)
  312 FORMAT (1H , 4X, I5, 5X, I5, 5X, I5)
  315. FORMAT (1H0)
  325 FORMAT (1H , 4X, I5, 5X, E15.7, 5X, E15.7, 5X, E15.7)
  335 FORMAT (1H , 4X, 'INITIAL STATE', /)
  336 FORMAT (1H , 4X, 'REPORTS AT EQUAL INTERVALS', /)
      END




      SUBROUTINE FNCT
      COMMON T, P, NR
      GO TO (5, 15), NR
    5 READ (5,303)  TX, PX
      WRITE (6,307)
      WRITE (6,310)  TX, PX
      SLOPE = PX / TX
      RETURN
   15 IF (T - TX)  25, 26, 26
   25 P = SLOPE * T
      RETURN
   26 P = PX
      RETURN
  303 FORMAT (4E15.7)
  307 FORMAT (1H , 4X, 'DATA FOR SUBPROGRAM  FNCT', /)
  310 FORMAT (1H , 4X, E15.7, 5X, E15.7)
      END
```

```
C          PROJECT 3258      R W NELSON     APRIL 25 1975
C          DEWATERING PROBLEM      CN METHOD (CN1 3258/2=874A)
C          VERSION 1
C              PART A, PRELIMINARIES
       DIMENSION POST(101), STEP(101), DSCN(101)
       DIMENSION A(100), B(100), C(100), OMEGA(100), DZ(100)
       COMMON L, LM1, A, B, C, OMEGA, DZ
       COMMON T, P
       COMMON X, QA, QB, QAP, QBP, CN, CU, QN, RHO, NR
       READ (5,301)  L, IND, MAX
       WRITE (6,310)
       WRITE (6,302)  L, IND, MAX
       WRITE (6,306)
       LP1 = L + 1
       LM1 = L - 1
       READ (5,303)  PREV, QLAM, QMT, TEST
       WRITE (6,311)  PREV, QLAM, QMT, TEST
       WRITE (6,307)
       NR = 1
       CALL SWIFT
       WRITE (6,307)
       CALL FNCT
       WRITE (6,307)
       NR = 2
       KTR = 0
       DO 5  I = 1, LP1
       POST(I) = PREV
     5 STEP(I) = PREV
       TEMP = L
       SAVE = QMT / TEMP
       DELT = SAVE * SAVE * QLAM
       T = DELT
       CALL FNCT
       POST(LP1) = P
       MARK = 0
       WRITE (6,335)
       TIME = 0.0
       TEMP = 0.0
       DO 3  I = 2, L
       SAVE = CN + CU * (STEP(I) ** QN)
       DSCN(I) = SAVE
     3 TEMP = TEMP + 1.0 / SAVE
       SAVE = CN + CU * (STEP(1) ** QN)
       DSCN(1) = SAVE
       TEMP = TEMP + 0.5 / SAVE
       SAVE = CN + CU * (STEP(LP1) ** QN)
       DSCN(LP1) = SAVE
       TEMP = TEMP + 0.5 / SAVE
    15 SAVE = L
       TEMP = TEMP * QMT / SAVE
       STORE = TEMP - QMT / RHO
       WRITE (6,325)  MARK, TIME, TEMP, STORE
       WRITE (6,306)
       DO 4  I = 1, LP1
       SAVE = DSCN(I) / RHO
     4 WRITE (6,325)  I, SAVE, STEP(I)
```

```
      WRITE (6,307)
      WRITE (6,336)
C                   PART B, CYCLE
  408 X = POST(1)
      CALL SWIFT
      B(1) = - 2.0 * (1.0 + QLAM * (QB + (POST(1) - POST(2)) * QBP))
      C(1) = 2.0 * QLAM * QB
      OMEGA(1) = - 2.0 * (QLAM * QB * POST(2) - (1.0 + QLAM * QB)
     1    * POST(1))
      X = STEP(1)
      CALL SWIFT
      OMEGA(1) = OMEGA(1) - 2.0 * (QLAM * QB * STEP(2)
     1    + (1.0 - QLAM * QB) * STEP(1))
      DO 405  I = 2, L
      X = POST(I)
      CALL SWIFT
      TEMP = POST(I+1) - POST(I-1)
      SAVE = TEMP * TEMP
      A(I) = QLAM * (QB - 0.5 * QA * TEMP)
      B(I) = - 2.0 * (1.0 + QLAM * QB) + 0.25 * QLAM * SAVE * QAP
     1    + QLAM * (POST(I+1) - 2.0 * POST(I) + POST(I-1)) * QBP
      C(I) = QLAM * (QB + 0.5 * QA * TEMP)
      STORE = - QLAM * (QB * (POST(I+1) + POST(I-1)) + 0.25 * QA * SAVE)
     1    + 2.0 * (1.0 + QLAM * QB) * POST(I)
      X = STEP(I)
      CALL SWIFT
      TEMP = STEP(I+1) - STEP(I-1)
      SAVE = TEMP * TEMP
      STORE = STORE - QLAM * QB * (STEP(I+1) + STEP(I-1))
      STORE = STORE - 2.0 * (1.0 - QLAM * QB) * STEP(I)
      OMEGA(I) = STORE - 0.25 * QLAM * QA * SAVE
  405 CONTINUE
      CALL TRI
      S = 0.0
      DO 406  I = 1, L
      TEMP = DZ(I)
      SAVE = POST(I)
      POST(I) = SAVE + TEMP
      TEMP = TEMP / SAVE
  406 S = S + TEMP * TEMP
      IF (S - TEST)  407, 408, 408
C                   PART C, OUTPUT
  407 KTR = KTR + 1
      IF (KTR - IND)  220, 221, 221
  221 KTR = 0
      MARK = MARK + IND
      TEMP = MARK
      TIME = TEMP * DELT
      TEMP = 0.0
      DO 701  I = 2, L
      SAVE = CN + CU * (POST(I) ** QN)
      DSCN(I) = SAVE
  701 TEMP = TEMP + 1.0 / SAVE
      SAVE = CN + CU * (POST(1) ** QN)
      DSCN(1) = SAVE
      TEMP = TEMP + 0.5 / SAVE
```

```
      SAVE = CN + CU * (POST(LP1) ** QN)
      DSCN(LP1) = SAVE
      TEMP = TEMP + 0.5 / SAVE
      SAVE = L
      TEMP = TEMP * QMT / SAVE
      STORE = TEMP - QMT / RHO
      WRITE (6,325)  MARK, TIME, TEMP, STORE
      WRITE (6,306)
      DO 251  I = 1, LP1
      STEP(I) = POST(I)
      SAVE = DSCN(I) / RHO
  251 WRITE (6,325)  I, SAVE, POST(I)
      WRITE (6,307)
      IF (MARK - MAX)  253, 432, 432
  432 CALL EXIT
  220 DO 202  I = 1, LP1
  202 STEP(I) = POST(I)
  253 TEMP = KTR + MARK + 1
      T = TEMP * DELT
      CALL FNCT
      POST(LP1) = P
      GO TO 408
C                 PART D, I/O ARRANGEMENTS
  301 FORMAT (3I5)
  302 FORMAT (1H , 4X, I5, 5X, I5, 5X, I5)
  303 FORMAT (4E15.7)
  306 FORMAT (1H )
  307 FORMAT (1H0)
  310 FORMAT (1H , 4X, 'DATA FOR MAIN PROGRAM', /)
  311 FORMAT (1H , 4X, E15.7, 5X, E15.7, 5X, E15.7, 5X, E15.7)
  325 FORMAT (1H , 4X, I5, 5X, E15.7, 5X, E15.7, 5X, E15.7)
  335 FORMAT (1H , 4X, 'INITIAL STATE', /)
  336 FORMAT (1H , 4X, 'REPORTS AT EQUAL INTERVALS', /)
      END




      SUBROUTINE SWIFT
      DIMENSION BLANKA(100), BLANKB(100), BLANKC(100), BLANKD(100)
      DIMENSION BLANKE(100)
      COMMON KLANK1, KLANK2, BLANKA, BLANKB, BLANKC, BLANKD, BLANKE
      COMMON BLANKF, BLANKG
      COMMON X, QA, QB, QAP, QBP, CN, CU, QN, RHO, NR
      GO TO (7, 1), NR
    7 READ (5,301)  QN, CN, CU, RHO
      READ (5,301)  B, COEFF, PARAM
      WRITE (6,302)
      WRITE (6,303)  QN, CN, CU, RHO
      WRITE (6,303)  B, COEFF, PARAM
      QNM1 = QN - 1.0
      QNM2 = QN - 2.0
      RETURN
    1 TEMP = ALOG(X)
      U = EXP(QN * TEMP)
```

```
      V = EXP(QNM1 * TEMP)
      W = EXP(QNM2 * TEMP)
      REGA = CN * CU * U
      REGC = REGA * QNM1 / (QN * CU * U)
      FRACT = REGA / RHO
      TEMP = FRACT * FRACT
      SAVE = TEMP * FRACT
      STORE = 1.0 + B * SAVE
      QH = COEFF * SQRT(FRACT) / STORE
      QK = REGA / (QN * CU * V)
      REGD = B * TEMP / STORE
      REGE = PARAM * QH * (0.5 / FRACT - 3.0 * REGD)
      REGF = PARAM * V
      REGF = REGF * REGF * QH
      QHP = REGE * V
      QKP = 1.0 - REGC
      QHPP = REGE * QNM1 * W + REGF * (-0.25 / TEMP + 18.0 * REGD * REGD
     1    - 9.0 * B * FRACT / STORE)
      QA = QK * QHP - QH
      QB = QK * QH
      QAP = QK * QHPP - REGC * QHP
      QBP = QK * QHP + QKP * QH
      RETURN
  301 FORMAT (4E15.7)
  302 FORMAT (1H , 4X, 'DATA FOR SUBPROGRAM  SWIFT', /)
  303 FORMAT (1H , 4X, E15.7, 5X, E15.7, 5X, E15.7, 5X, E15.7)
      END




      SUBROUTINE TRI
      DIMENSION A(100), B(100), C(100), R(100)
      DIMENSION BETA(100), GAMMA(100), DZ(100)
      COMMON L, LM1, A, B, C, R, DZ
      COMMON BLANKF, BLANKG
      COMMON BLANK1, BLANK2, BLANK3, BLANK4, BLANK5, BLANK6, BLANK7,
     1      BLANK8, BLANK9, KLANKH
      BETA(1) = B(1)
      GAMMA(1) = R(1) / B(1)
      DO 505  I = 2, L
      BETA(I) = B(I) - A(I) * C(I-1) / BETA(I-1)
  505 GAMMA(I) = (R(I) - A(I) * GAMMA(I-1)) / BETA(I)
      DZ(L) = GAMMA(L)
      DO 506  I = 1, LM1
      J = L - I
  506 DZ(J) = GAMMA(J) - C(J) * DZ(J+1) / BETA(J)
      RETURN
      END
```

```
C           ALTERNATIVE ARRANGEMENT OF SUBPROGRAM  FNCT
C           FOR CARD INPUT OF APPLIED LOAD SCHEDULE
      SUBROUTINE FNCT
      DIMENSION BLANKA(100), BLANKB(100), BLANKC(100), BLANKD(100)
      DIMENSION BLANKE(100)
      COMMON KLANK1, KLANK2, BLANKA, BLANKB, BLANKC, BLANKD, BLANKE
      COMMON T, P
      COMMON BLANK1, BLANK2, BLANK3, BLANK4, BLANK5, BLANK6, BLANK7,
     1     BLANK8, BLANK9, NR
      GO TO (5, 15), NR
    5 READ (5,303)  TINIT, PINIT
      READ (5,303)  TX, PX
      SLOPE = (PX - PINIT) / (TX - TINIT)
      RETURN
   15 IF (T - TX)  35, 36, 37
   35 P = PINIT + SLOPE * (T - TINIT)
      RETURN
   36 P = PX
      RETURN
   37 TINIT = TX
      PINIT = PX
      READ (5,303)  TX, PX
      SLOPE = (PX - PINIT) / (TX - TINIT)
      GO TO 15
  303 FORMAT (E15.7, 15X, E15.7)
      END
```

```
C          TEMPORARY MAIN PROGRAM
      DIMENSION A(100), B(100), C(100), R(100)
      DIMENSION BETA(100), GAMMA(100), DZ(100)
      COMMON L, LM1, A, B, C, R, DZ
      COMMON BLANKF, BLANKG
      COMMON BLANK1, BLANK2, BLANK3, BLANK4, BLANK5, BLANK6, BLANK7,
     1     BLANK8, BLANK9, KLANKH
      L = 7
      LM1 = L - 1
      B(1) = 1.0
      C(1) = 5.0
      R(1) = 6.0
      A(2) = 2.0
      B(2) = 1.0
      C(2) = - 4.0
      R(2) = - 1.0
      A(3) = 1.0
      B(3) = 1.0
      C(3) = 1.0
      R(3) = 3.0
      A(4) = 2.0
      B(4) = 3.C
      C(4) = - 2.0
      R(4) = 3.0
      A(5) = - 1.0
      B(5) = 2.0
      C(5) = 5.0
      R(5) = 6.0
      A(6) = 0.C
      B(6) = 4.0
      C(6) = 7.0
      R(6) = 11.0
      A(7) = 6.0
      B(7) = 1.0
      R(7) = 7.0
      CALL TRI
      DO 7  I = 1, L
    7 WRITE (6,301) DZ(I)
      CALL EXIT
  301 FORMAT (1H , 4X, E15.7)
      END
```

```
C            SUBPROGRAM FOR SOLUTION OF TRIDIAGONAL SYSTEM
C                 (TRI 3258/3=875A)
      SUBROUTINE TRI
      DIMENSION A(100), B(100), C(100), R(100)
      DIMENSION BETA(100), GAMMA(100), DZ(100)
      COMMON L, LM1, A, B, C, R, DZ
      COMMON BLANKF, BLANKG
      COMMON BLANK1, BLANK2, BLANK3, BLANK4, BLANK5, BLANK6, BLANK7,
     1      BLANK8, BLANK9, KLANKH
      BETA(1) = B(1)
      GAMMA(1) = R(1) / B(1)
      DO 505  I = 2, L
      BETA(I) = B(I) - A(I) * C(I-1) / BETA(I-1)
  505 GAMMA(I) = (R(I) - A(I) * GAMMA(I-1)) / BETA(I)
      DZ(L) = GAMMA(L)
      DO 506  I = 1, LM1
      J = L - I
  506 DZ(J) = GAMMA(J) - C(J) * DZ(J+1) / BETA(J)
      RETURN
      END
```